Computational techniques for optimization of subthalamic nucleus deep brain stimulation in the context of Parkinson's disease

Undergraduate Research Thesis

Presented in partial fulfillment of the requirements for graduation
with honors research distinction in Neuroscience in the
undergraduate colleges of The Ohio State University

by

Peter Josh Hamer

The Ohio State University
July 2015

Project Advisor: Professor Per Sederberg, Department of Psychology

SPONSORSHIP

2015 College of Arts and Sciences Undergraduate Research Scholarship
Ohio State University Colleges of Arts & Sciences

2015 Social and Behavioral Sciences Undergraduate Research Grant
Ohio State Department of Social & Behavioral Sciences

2014 University Honors & Scholars Summer Research Fellowship
Ohio State University Honors & Scholars

ACKNOWLEDGEMENTS

Dylan M. Nielson, PhD
Department of Neurological Surgery, Center for Neuromodulation, The Ohio State University Wexner Medical Center

Per B. Sederberg, PhD
Department of Psychology, The Ohio State University

Ali R. Rezai, MD
Department of Neurological Surgery, Center for Neuromodulation, The Ohio State University Wexner Medical Center

INTRODUCTION

Deep brain stimulation has been successfully used in the treatment of Parkinson's disease for more than two decades, with deep brain stimulation of the subthalamic nucleus significantly improving motor function. Symptoms of the disease (e.g., tremor, rigidity, bradykinesia) are measured by the Unified Parkinson's Disease Rating Scale Part III, but uncertainty remains concerning the areas in and around the subthalamic nucleus that are associated with each particular symptoms included in UPDRS-III. Here, we retrospectively examine a cohort of Parkinson's patients implanted at the Center for Neuromodulation in the Ohio State Wexner Medical Center. By combining anatomically-detailed pre-operative magnetic resonance imaging with post-operative computed tomographic imaging, we accurately determine the actual location of implanted electrode leads, then model a volume of tissue activation around each electrode to estimate the neuronal cell bodies and fiber tracts that are most likely to be affected by the stimulation parameters (i.e., voltage, pulse width, and frequency) that are programmed by clinicians during follow-up. By correlating these volumes of tissue activation with each motor function subscore, we have built three-dimensional statistical and probabilistic maps in and around the subthalamic nucleus that will allow clinicians to target lead placement and stimulation to particular deep brain regions based on patient-specific symptoms.

PARKINSON'S DISEASE

OVERVIEW

Approximately 60,000 new Parkinson's disease (PD) diagnoses are made each year in the United States, and disease prevalence for those over 65 years of age is estimated to be 950 per 100,000 (Hirtz et al., 2007). First described by James Parkinson in 1817 in his "Essay on the Shaking Palsy," between 4–6 million people worldwide suffer from the disease (parkinson.org), making it the second most common neurodegenerative disease after Alzheimer's (Wirdefeldt et al., 2011). Cardinal symptoms of the idiopathic disease include motor, autonomic, psychiatric, and cognitive dysfunction, all of which play a role in severely debilitating the lives of those afflicted.

SYMPTOMS

Motor

Diagnostic criteria (at least 2 of 3):

- ❖ resting tremor in appendicular and/or orofacial muscles at 4–6 Hz
- ❖ bradykinesia
- ❖ rigidity of arms, legs, trunk

Other:

- ◆ akinesia
- ◆ postural reflex impairment, leading to instability and retropulsion
- ◆ stooped posture
- ◆ shuffling gait
- ◆ freezing gait
- ◆ masked facial expression (i.e., hypomimia)
- ◆ hypophonia
- ◆ micrographia

Autonomic

- ◆ paresthesias (e.g., 'pins and needles', tingling, burning)
- ◆ seborrheic dermatitis, leading to dandruff
- ◆ hypotension, including orthostatic hypotension
- ◆ constipation
- ◆ erectile dysfunction in men
- ◆ early satiety when eating
- ◆ decreased reflexive blinking and swallowing
- ◆ hyperhidrosis
- ◆ urinary urgency, frequency, and incontinence
- ◆ sialorrhea due to slowed swallowing

Psychiatric
- depression, including anhedonia
- anxiety
- irritability
- psychosis, including hallucinations

Cognitive
- attention deficits
- memory impairment
- visuospatial impairment
- endorsement of slowed processing
- dementia

Symptoms preceding motor dysfunction
- anosmia
- sleep disturbances, including REM behavior disorder

ETIOLOGY

Epidemiological studies have indicated a role for both genetic and environmental factors in pathogenesis of the disease. Distinct genes appear to be involved in familial versus sporadic disease, and diet/lifestyle choices, as well as occupational exposures, may positively or negatively impact an individual's risk of developing PD (Wirdefeldt et al., 2011). While the biomolecular mechanisms that lead to striatal neurodegeneration are being elucidated by virtue of such epidemiological findings, the ostensibly complex etiology of PD eludes rigorous description in the literature.

Theories exist concerning PD origins in defective protein handling, mitochondrial dysfunction, oxidative stress, and inflammation (Wirdefeldt et al., 2011), but clinical treatment of the disease has yet to see dramatic improvements as a result of these insights. Neither adequate diagnostic biomarkers nor sophisticated pharmacological interventions currently exist for PD.

MOTOR EXAMINATION

UNIFIED PARKINSON'S DISEASE RATING SCALE - PART III
(Fahn et al., 1987)

18. Speech
0 = Normal.
1 = Slight loss of expression, diction and/or volume.
2 = Monotone, slurred but understandable; moderately impaired.
3 = Marked Impairment, difficult to understand.
4 = Unintelligible.

19. Facial Expression
0= Normal.
1 = Minimal hypomimia, could be normal "Poker Face."
2 = Slight but definitely abnormal diminution of facial expression.
3 = Moderate hypomimia; lips parted some of the time.
4 = Masked or fixed face with severe or complete loss of facial expression; lips parted ¼ inch or more.

20. Tremor at Rest (Face, lips, chin, head, upper and lower extremities.)
0 = Absent.
1 = Slight and infrequently present.
2 = Mild in amplitude and persistent. Or moderate in amplitude, but only intermittently present.
3 = Moderate in amplitude and present most of the time.
4 = Marked in amplitude and present most of the time.

21. Action or Postural Tremor of Hands
0 = Absent.
1 = Slight; present with action.
2 = Moderate in amplitude, present with action.
3 = Moderate in amplitude with posture holding as well as action.
4 = Marked in amplitude; interferes with feeding.

22. Rigidity (Neck, upper and lower extremities. Judged on passive movement of major joints with patient relaxed in sitting position. Cogwheeling to be ignored.)

0 = Absent.
1 = Slight or detectable only when activated by mirror or other movements.
2 = Mild to moderate.
3 = Marked, but full range of motion easily achieved.
4 = Severe, range of motion achieved with difficulty.

23. Finger Taps (Patient taps thumb with index finger in rapid succession.)
0 = Normal.
1 = Mild slowing and/or reduction in amplitude.
2= Moderately impaired. Definite and early fatiguing. May have occasional arrests in movement.
3 = Severely impaired. Frequent hesitation in initiating movements or arrests in ongoing movement.
4 = Can barely perform the task.

24. Hand Movements (Patient opens and closes hands (Pronation-supination movements of hands, vertically and horizontally, with as large an amplitude as possible, both hands simultaneously.)
0 = Normal.
1 = Mild slowing and/or reduction in amplitude.
2= Moderately impaired. Definite and early fatiguing. May have occasional arrests in movement.
3 = Severely impaired. Frequent hesitation in initiating movements or arrests in ongoing movement.
4 = Can barely perform the task.

25. Rapid Alternating Movements of Hands (Pronation-supination movements of hands, vertically and horizontally, with as large an amplitude as possible, both hands simultaneously.)
0 = Normal.
1 = Mild slowing and/or reduction in amplitude.
2 = Moderately impaired. Definite and early fatiguing. May have occasional arrests in movement.
3 = Severely impaired. Frequent hesitation in initiating movements or arrests in ongoing movement.
4 = Can barely perform the task.

26. Leg Agility (Patient taps heel on the ground in rapid succession picking up entire leg. Amplitude should be at least 3 inches.)

0 = Normal.
1 = Mild slowing and/or reduction in amplitude.
2= Moderately impaired. Definite and early fatiguing. May have occasional arrests in movement.
3 = Severely impaired. Frequent hesitation in initiating movements or arrests in ongoing movement.
4 = Can barely perform the task.

27. Arising from Chair (Patient attempts to rise from a straightbacked chair, with arms folded across chest.)

0 = Normal.
1 = Slow; or may need more than one attempt.
2 = Pushes self up from arms of seat.
3 = Tends to fall back and may have to try more than one time, but can get up without help.
4 = Unable to arise without help.

28. Posture

0 = Normal erect.
1 = Not quite erect, slightly stooped posture; could be normal for older person.
2 = Moderately stooped posture, definitely abnormal; can be slightly leaning to one side.
3 = Severely stooped posture with kyphosis; can be moderately leaning to one side.
4 = Marked flexion with extreme abnormality of posture.

29. Gait

0 = Normal.
1 = Walks slowly, may shuffle with short steps, but no festination (hastening steps) or propulsion.
2 = Walks with difficulty, but requires little or no assistance; may have some festination, short steps, or propulsion.
3 = Severe disturbance of gait, requiring assistance.
4 = Cannot walk at all, even with assistance.

30. Postural Stability (Response to sudden, strong posterior displacement produced by pull on shoulders while patient erect with eyes open and feet slightly apart. Patient is prepared.)

0 = Normal.
1 = Retropulsion, but recovers unaided.
2 = Absence of postural response; would fall if not caught by examiner.
3 = Very unstable, tends to lose balance spontaneously.
4 = Unable to stand without assistance.

31. Body Bradykinesia and Hypokinesia (Combining slowness, hesitancy, decreased arm swing, small amplitude, and poverty of movement in general.)

0 = None.
1 = Minimal slowness, giving movement a deliberate character; could be normal for some persons. Possibly reduced amplitude.
2 = Mild degree of slowness and poverty of movement which is definitely abnormal. Alternatively, some reduced amplitude.
3 = Moderate slowness, poverty or small amplitude of movement.
4 = Marked slowness, poverty or small amplitude of movement.

TREATMENT

The symptomatic treatment of Parkinson's disease (PD) is primarily pharmacological in nature and is prescribed to minimize motor and non-motor symptoms. Medical treatment options include various dopaminergic options, such as the dopamine precursor, levodopa, with or without agents to increase peripheral availability of the precursor via decarboxylase or catechol-*O*-methyl transferase inhibition; dopamine agonists such as pramipexole, ropinirole, and rotigotine; and monoamine oxidase B inhibitor such as rasagiline and selegiline. These may be combined with non-dopaminergic medications, such as benztropine mesylate and trihexyphenidyl, both of which have anticholinergic activity.

In many cases, pharmacological therapy is unable to provide satisfactory symptom control as the disease progresses and patients may develop disabling side effects after long-term use of PD medications (Stocchi et al., 2008). As neurodegeneration progresses, medications may provide shorter and shorter periods of symptom relief, requiring larger and larger doses that precipitate debilitating dyskinesias. When this stage of PD is reached, surgical treatment may be indicated to provide relief of symptoms and allow for simplification and/or reduction of medication therapies.

DBS

HISTORY

Descriptions of surgical treatment for PD date back to the first half of the 20th century, and focus primarily on ablative procedures. This approach abated somewhat with the introduction of dopaminergic pharmacological interventions, such as levodopa, but made a resurgence in the 1990s (Bronstein et al., 2011). By the beginning of the 21st century, however, ablative lesioning was by and large abandoned for the functional lesioning made possible by electrical stimulation, which has the crucial advantage of being revisable and adjustable. The new technique, known as deep brain stimulation (DBS), was applied to novel subcortical structures, and the STN became one of the most commonly targeted deep nuclei in the treatment for PD (Bergman et al., 1990; DeLong 1990; Aziz et al., 1991). Since the U.S. Food and Drug Administration approved DBS for the treatment of PD in 2002, more than 100,000 implants have been placed throughout the world, according to Medtronic Inc., a leading manufacturer of DBS technologies.

PROCEDURE

Although proven safe and effective, DBS therapy is most effective when applied to the correctly selected PD patient (Bronstein et al., 2011), and nearly one-third of DBS failures are attributed to improper patient selection (Okun et al., 2005). In the most expert neurological centers, multidisciplinary teams of neurologists, neurosurgeons, neuropsychologists, and even psychiatrists evaluate a patient's candidacy for surgery, determining their individual risk-benefit analysis. It is worth noting, however, that there is evidence that DBS interventions (for patients with non-atypical parkinsonism) may have a greater positive impact on quality of life measures when delivered in earlier stages of Parkinson's disease progression (Schüpbach et al., 2007; Merola et al., 2015).

After pre-screening, baseline assessments are scheduled where, among other measures, UPDRS-III scores are collected after an approximately 12 hour washout of PD medications, then after a PD medication dose at maximum pharmacological efficacy, which is typically achieved 45–90 minutes after oral ingestion. Experts agree that a 30% improvement in UPDRS-III score with dopaminergic medications is the single-best predictor of a patient's response to DBS (Charles et al., 2002; Kleiner-Fisman et al., 2006).

If cleared for the procedure, the day of surgery involves standard surgical preparation in addition to stereotactic head-frame placement in institutions that use frame-based navigation systems. After the frame is attached to the patient's skull, neuroimaging data is gathered (via MRI, CT, ventriculography, or some combination of these technologies), then fed into specialized, interactive neurosurgical planning software which allows the surgical team to find

implantation trajectories that reach the subcortical target while avoiding major blood vessels and the sulci of the cortex.

With multiple trajectories in mind, the surgeon creates a burr hole that provides access for the slow insertion of a microelectrode down to target. During this process, electrophysiologists monitor the electrical activity recorded by the microelectrode to verify correct placement. The basal ganglia nuclei in the immediate vicinity of the STN display consistent baseline firing patterns, as well as predictable responses to active and passive movement of the patient's appendicular and orofacial muscles. For this reason, many functional neurosurgeons prefer to perform at least part of their DBS procedures on awake and alert patients.

To aide in targeting, supratherapeutic doses of electrical stimulation are applied to identify areas associated with side effects (e.g., paresthesias, involuntary muscle contractions, autonomic responses), which must be avoided, and areas associated with reduction in PD motor symptoms. Once the surgical team reaches a consensus vis-à-vis the optimal location for stimulation, the microelectrode is removed and replaced with the DBS lead.

Following a final round of electrophysiological verification with the final implant, the entire procedure may be repeated on the contralateral brain hemisphere, if appropriate and determined in advance, and intraoperative neuroimaging, by way of MRI or CT, is completed. If DBS lead locations are acceptable to the neurosurgeon and evaluation of hemorrhage or pneumocephalus is normal, the skull and skin incisions are closed, the stereotactic frame is removed, and the patient is sent to recovery. Depending on the patient's condition, implantation of the internal pulse generator into the infraclavicular space of the external chest wall or the abdomen, with subsequent subcutaneously-tunneled, wired connections to the DBS lead, may be performed during the same hospitalization or completed within days or weeks. For elderly patients or those with certain conditions (e.g., cognitive impairment), contralateral implantation of a second DBS lead and internal pulse generator may be scheduled within one month. It should be noted, however, that adequate relief of PD symptoms is often achieved with unilateral neurostimulation.

Incidence of surgical complications varies by source and may include intracranial hemorrhage (0–10%), stroke (0–2%), infection (0–15%), lead erosion without infection (1–2.5%), lead fracture (0–15%), lead migration (0–19%), and death (0–4.4%) (Weaver et al., 2009; Blomstedt & Hariz, 2005; Videnovic & Metman, 2008; Hamani & Lozano, 2006; Deuschl et al., 2006), although advances in technology and technique are continuously reducing these figures (Bronstein et al., 2011).

TITRATION

Postoperative care focuses on the titration of stimulation parameters to

achieve maximal efficacy. Typical parameters for STN-DBS in PD involving a monopolar configuration include voltages between 2.5–3.5 V, pulse widths of 60–90 μs, and frequencies of 130–180 Hz. These may be exceeded if doing so lessens the severity of symptoms without causing side effects, which include sensory and motor changes such as involuntary contraction of face, arm, and leg muscles, dysarthritic speech, dystonic posturing, spontaneous eye deviation, as well as changes in heart rate, blood pressure, and respiratory rate. It is also critical not to exceed a total charge density of 30 μcoulomb/cm^2, since the application of electrical stimulation above this threshold may lead to tissue damage.

Because each DBS lead is equipped with 4 electrode contacts, the clinician (i.e., neurologist, neurosurgeon, nurse, or physician assistant) may test the efficacy of a given monopolar configuration with the internal pulse generator serving as anode and any of the four contacts serving as cathode. In some cases, bipolar configurations, wherein the anode is the internal pulse generator and the cathode comprises 2 electrode contacts, produce the best results; in others, interleaving stimulation, involving alternating pulses from 2 unique configurations, is optimal (Moreau et al., 2008). With the help of intraoperative neurophysiological data and postoperative imaging, the clinician systematically evaluates the adverse and beneficial effects of a wide range of possible configurations and stimulation parameters, and typically achieves optimum settings within 4–5 titration sessions over 3–6 months (Bronstein et al., 2011). Once set, the neurostimulator is typically active at these parameters 24 hr/day, with some patients receiving instructions for slight adjustments in stimulation at home as needed.

Side effects of DBS for movement disorders include: suicidal ideation, depression, gastrointestinal disturbances, nausea, muscle weakness or partial paralysis, jolting or shocking sensation, numbness, paresthesias, facial flushing and motor contraction, dizziness, headaches pain, changes in vital signs, hyperactivity or euphoria, pain or discomfort, dry mouth, itching at the surgical site, insomnia, increased fatigue, cognitive disturbance, restlessness, weight gain or loss, speech and visual difficulties, blurred or double vision, unusual smell and taste sensations, cognitive and/or behavioral changes, mood changes, and energy level changes (Rezai et al., 2008).

During titration sessions, PD patients are evaluated for the possible side effects of DBS and undergo a variety of other clinical assessments, including UPDRS-III, following a PD medication washout period. This ensures that the effects of DBS are readily observable and that clinician-initiated changes in stimulation parameters may be associated with changes in motor function.

Importantly, the stimulation parameters selected impact on the life of the internal pulse generator's battery, which is typically removed and replaced intraoperatively every 2–5 years, although inductive-rechargeable batteries that last up to 9 years are available. When surgical lead placement is suboptimal or excessive lead migration occurs, higher levels of stimulation are required for adequate therapeutic effects, resulting in premature depletion of the implanted

battery.

SUCCESSES

Patients undergoing DBS have obtained significant improvements in overall functioning, independence, quality of life enhancement, return to work or school and resumption of daily activities (Machado et al., 2006; Rezai et al., 2008; Malone et al., 2009). Two large clinical trials found STN neurostimulation to be superior in treating the motor complications of advanced Parkinson's therapy compared to best medical management alone (Deuschl et al., 2006; Weaver et al., 2009)

LIMITATIONS

Evidence from case studies and retrospective meta-analyses suggests that STN-DBS may lead to a variety of neuropsychological sequelae (e.g., mania, apathy, depression, suicidal ideation, impulsivity, attentional impairment, or memory deficits) (Voon et al., 2006; Parsons et al., 2006; Temel et al., 2006), but well-controlled studies report that the only consistent neuropsychological side effects of STN-DBS are impairments in verbal fluency and Stroop (i.e., an executive control task) performance (Voon et al., 2006; Obeso et al., 2011; Jahanshahi et al., 2000; Witt et al., 2004; Witt et al., 2006; Witt et al., 2013; Schroeder et al., 2002; Brittain et al., 2012).

Standard therapeutic stimulation parameters of monopolar cathodic, 1–5 V, 60–200 ms, and 120–180 Hz were determined primarily by trial and error (Rizzone et al., 2001; Moro et al., 2002; Volkmann et al., 2002; O'Suilleabhain et al., 2003) and postoperative titration remains an empirical exercise. This lack of understanding upsets the extension of DBS to patient populations that have few, if any, reliable treatment options.

BASAL GANGLIA

PHYSIOLOGY

The basal ganglia comprise subcortical nuclei with functions in distributed networks that modulate activity in motor, premotor, dorsolateral, anterior cingulate, and frontal eye field cortices (reviewed in Volkmann et al., 2010).

The largest basal ganglia nucleus, the striatum, is associated with facilitated and suppressed states that are determined by the strength of cortical input, and is thought to act as a filter to increase signal-to-noise ratio (da Cunha et al., 2015). Striatal potentiation state is also determined by dopaminergic input from the substantia nigra pars compacta (SNpc), which can prevent transitions from suppressed to facilitated (da Cunha et al., 2015). In this way, the striatum integrates cortical and subcortical input (Bolam et al., 2000; Nambu et al., 2000; Miwa et al., 2001; Jaeger and Kita, 2011; Obeso et al., 2013; Surmeier, 2013; Ullsperger et al., 2014; Woolley et al., 2014), which is projected to the globus pallidus, whose internal segment serves as the major output structure of the basal ganglia. Basal ganglia output via the internal segment of the globus pallidus (GPi) gates thalamic activity, resulting in facilitation and suppression of cortical activity (reviewed in Wiecki & Frank, 2013). Thus, networks that include the basal ganglia play a role in the selection, facilitation, and inhibition of action, emotion, and cognition (reviewed in Volkmann et al., 2010).

The STN is the only excitatory nucleus in the basal ganglia (Nambu et al., 2002), and receives input from frontal areas involved in inhibition and executive control (reviewed in Jahanshahi, 2013) as well as subcortical input. Output to the GPi from the STN can suppress the gating of thalamic activity, resulting in decreased cortical activity (reviewed in Frank, 2006).

Importantly, the STN can be anatomically subdivided into functionally distinct regions (e.g., oculomotor, associative, limbic, and somatomotor) and cortico-subthalamic projections reflect this segregated, topographical organization (Afsharpour, 1985; Hartmann-von Monakow et al., 1978). However, the dendrites of STN neurons extend up to 1200 μm and so there may be considerable convergence of inputs from different cortical areas onto a single neuron in the STN (Yelnik & Percheron, 1979).

In general, the dorsolateral subregion of the STN is relevant to somatomotor networks (Coyne et al., 2006), while the ventral subregion is relevant to associative and limbic processes (Alexander & Crutcher, 1990; Joel & Weiner, 1997; Karachi et al., 2005; Parent & Hazrati, 1995; Temel et al., 2005). This mirrors the segregation of motor and associative circuits found in other cortical and subcortical regions (Bevan et al., 2006; Romanelli et al., 2005), which enables parallel processing across multiple domains (Alexander & Crutcher, 1990).

Neuronal oscillations reflect the synchronized activity of neuronal ensembles. Cortical gamma-band (~40–400 Hz) amplitude is increased (as the blood-oxygen level) during motor, visual, language, and cognitive tasks (Scheeringa et al., 2011) and is thought to reflect summed asynchronous spiking

activity (Manning et al., 2009). Abnormal inhibition of the cortical areas to which the BG project, including motor regions, is thought to explain the suppression of motor activity and impairment in motor sequencing observed in PD (Dubois et al., 1991; Willingham, 1998; de Hemptinne et al., 2013; Young & Penney, 1993).

In PD, pathological beta-band (13–30 Hz) neuronal synchronization seems to occur in the basal ganglia (Hammond et al., 2007; Levy et al., 2000; Nini et al., 1995) and specifically in the STN (Levy et al., 2002; Kuhn et al., 2005; Weinberger et al., 2006; Moran et al., 2008). Moreover, it appears that the pathological signal is locally generated in the STN (Kuhn et al., 2005, Levy et al., 2002)

Suppression of this beta power in the STN using 2 standard treatments for PD, levodopa or DBS, is correlated with improvements in bradykinesia and rigidity (Kuhn et al., 2006; Weinberger et al., 2006; Kuhn et al., 2009; Ray et al., 2008). Therapeutic effects of DBS of the STN in PD are also correlated with a reduction of beta-band activity in the motor circuitry (Kuhn et al., 2008).

Reduction in tremor severity, on the other hand, is associated with decreases in low gamma (31–45 Hz) oscillations in the STN (Anzak et al., 2012). Both tremor amplitude and low gamma activity are suppressed by application of electrical stimulation, although reduction of tremor lags the reduction in gamma by several seconds and reemerges later than gamma increase after stimulation is discontinued (Beudel et al., 2015). Interestingly, low gamma activity in the STN is increased with cognitive load (Anzak et al., 2011; Anzak et al., 2013), which also increases resting tremor in PD patients (Deuschl et al., 1998).

Stimulation of limbic subregions of the STN may explain the experience of hypomanic and manic states following DBS (Mallet et al., 2007; Mandat et al., 2006; Raucher-Chene et al., 2008). Studies have shown that stimulation in this region changes activation patterns in thalamic and cortical regions that are relevant to affect, while stimulation in more-dorsal regions of the STN result in motor network activation (Mallet et al., 2007). Additionally, there is evidence that DBS impairs the ability to recognize fearful content in faces and film sequences (Biseul et al., 2005; Vicente et al., 2009).

OBJECTIVE

The current method of deep brain stimulation programming requires frequent clinical visits for adjustment of programming, which extends over a period of months. Stimulation titration is guided primarily by clinician impression, and the lack of objective methods for determining optimum parameters ensures that the process remains time-consuming. By providing the clinician with visualizations of patient-specific electrode location, models of tissue activation, and statistical data regarding efficacy at various stimulation locations, follow-up for DBS therapy could be simplified and even improved. In this study, we describe a computational pipeline for creation of such visualizations.

METHODS

SUBJECTS

Subjects include patients with idiopathic PD undergoing unilateral STN-DBS therapy (right: n = 15; left: n = 33) at the Center for Neuromodulation at The Ohio State University Wexner Medical Center (OSUWMC). All subjects provided informed consent for participation in the Atlas Protocol, in which demographic and clinical data was deidentified and stored in a secured database for subsequent study. In this retrospective analysis, the data collected includes preoperative neuroimaging, preoperative UPDRS-III assessments, postoperative neuroimaging, postoperative UPDRS-III assessments, stimulation parameters at follow-up visits for titration, and charted descriptions of adverse events.

Patients with significant comorbidities do not receive DBS treatment and are thus excluded from the database. Additional exclusion criteria for this study include the experience of significant adverse events including surgical or device complications (e.g., hemorrhage or severe infection requiring hospitalization or prolongation of existing hospitalization, lead fracture or other failures leading to surgical explantation or revision); significant cognitive impairment or dementia; uncontrolled depression, anxiety, or other mood disorder. Participants are also free to terminate their participation in the study at any time.

All implantations were performed at OSUWMC between 2010–2015, using Medtronic Neurological DBS leads (model 3389) and frame-based stereotactic technique with preoperative magnetic resonance neuroimaging. Post-implantation, lead locations were verified with in-suite CT. Follow-up visits include UPDRS-III assessment in the unmedicated state with stimulation turned on.

COMPUTATIONAL APPROACH

An important goal of this study is to create a computational pipeline that utilizes clinical data (generally, outcome measures, neuroimaging, and neurostimulation parameters) to create statistical maps that will delineate the relationship between stimulated structures and clinical efficacy.

To accomplish this, we normalize patient-specific neuroimaging data to the Montreal Neurological Institute 152 standard brain (Grabner et al., 2006) nonlinear/nonrigid tools available in the open-source neuroimaging software packages AFNI (Cox, 2011) and FSL (Smith et al., 2004). These measure overall image mismatch and provide a minimization algorithm that progressively optimizes a 4 × 4 transformation matrix by first translating, rotating, scaling, and shearing the reference volume, and subsequently warping with nonlinear operations to align the volumes in fine morphological detail.

After modeling the subject anatomy in standard space, preoperative MRIs from each patient are coregistered with the postoperative CT using CRAnialVault Explorer (CRAVE) (D'Haese et al., 2012), which automatically extracts the x, y, z coordinates in subject space for the 4 electrode contacts on each DBS lead. We then apply the transformation matrix to the coordinates of the DBS leads to visualize in standard space.

Using open-source analytical tools available in the Python programming language (van Rossum, 1995), we programmatically extract clinical outcome and titration data from the Atlas Database. In CRAVE, the stimulation parameters active during UPDRS-III assessments are masked into estimated volumes of tissue activation (VTAs), which are modeled at the appropriate electrode contact in subject space. We transform the VTA to standard space, as described above, and weight each voxel according to the reported change in UPDRS-III subscore, scaling by the number of subjects contributing to each voxel.

By combining the neuroimaging and clinical data acquired from the large sample in the Atlas Database, we create statistical maps that can display trends in the relationship between subscore outcomes and stimulation location.

To produce probabilistic maps that enable prediction of optimal stimulation locations, we extract x, y, z, and scaled outcome measures from each 4 dimensional statistical map. We test these terms for predictive ability in a generalized linear model (GLM) with the following equation:

$$\begin{aligned}\text{scaled outcome} \sim\ & x + y + z + x{:}y + y{:}z + x{:}z + x{:}y{:}z + \\ & x^2 + y^2 + z^2 + x^2{:}y^2 + y^2{:}z^2 + x^2{:}z^2 + x^2{:}y^2{:}z^2 + \\ & x^3 + y^3 + z^3 + x^3{:}y^3 + y^3{:}z^3 + x^3{:}z^3 + x^3{:}y^3{:}z^3 + \\ & x^4 + y^4 + z^4 + x^4{:}y^4 + y^4{:}z^4 + x^4{:}z^4 + x^4{:}y^4{:}z^4\end{aligned}$$

The GLM builds a manifold with its predictions, wherein each 1 mm^3 voxel contributes positively or negatively to an estimated change in outcome if it is included in the VTA at a given stimulation parameterization.

We judge the success of the model by calculating Pearson's product-moment correlation coefficient, first for all predictions made vs. actual outcomes for each subject independently to identify potential subject-level issues arising from pipeline processing failures. Then, we assess performance of the model in UPDRS-III subscore prediction across all of the data learned by each subscore manifold.

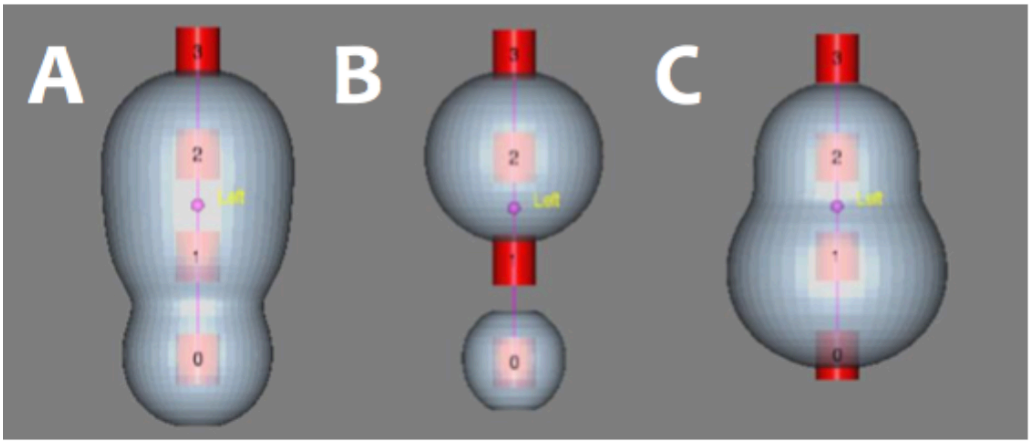

Figure 1. Sample VTA masks specified by stimulation parameters recorded at three visits. A: [0+/1-/2-] 3.0 V, 120 μs, 150 Hz. B: [0+/2-] 2.0 V, 60 μs, 150 Hz. C: [2+/1-] 3.6 V, 130 μs, 185 Hz.

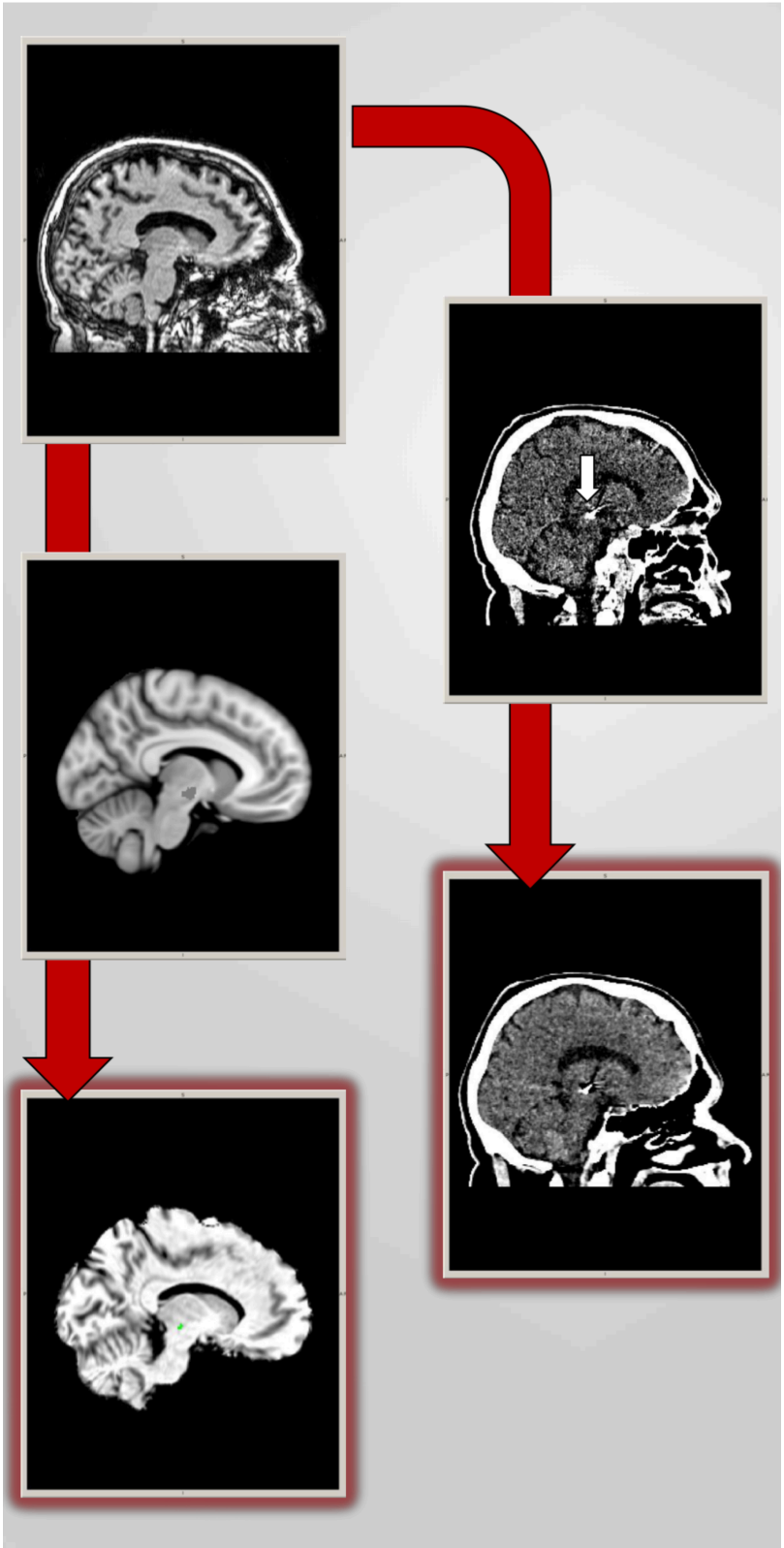

Figure 2. Pre-operative MRI for subject 120 captures anatomical detail.

Figure 3. Post-operative CT for subject 120 reveals location of DBS leads (white arrow).

Figure 4. Montreal Neurological Institute standard brain created using 152 subjects.

Figure 5. Co-registration of CT to MRI. DBS lead location can thus be determined accurately in MRI space.

Figure 6. MRI of subject 120, normalized to standard brain to allow between-subject comparisons of anatomical data.

RESULTS

The results of the subject-level examination of probabilistic manifold accuracy are shown in Table 1. In this iteration of the pipeline, the highest correlations between actual and predicted outcomes are seen for subject 66 (r = 0.997), who is undergoing right hemisphere STN-DBS, and subject 191 (r = 0.997), who is receiving stimulation in the left STN. Predictions made for these individuals derive from the model's instruction on fewer than 20 observations (for subject 66, n = 17; for subject 191, n = 18). In the case of these two subjects, model predictions underestimate the outcome: predictions for subject 66 are 85% less than actual outcome, while predictions for subject 191 are 66% less than actual outcome.

Predictions made concerning UPDRS-III outcomes for subject 129, who is implanted at the left STN, are least correlated with the actual outcomes (r = 0.063, n = 11), with similar model divergence observed for subject 65 (left-implanted, r = 0.162), who contributed 63 observations to the instruction of the model. Although probabilistic manifolds for 40 out of 48 subjects correlate positively with actual outcomes at r > 0.600, predictions for subject 1 (right STN-DBS patient) and subject 48 (left STN-DBS patient) are negatively correlated with actual outcomes (respectively, r = -0.575, n = 14 and r = -0.135, n = 10).

Table 2 displays the performance of the model on the subscore-level for observations involving right-implanted subjects. Predictions for tremor at rest of the face, arising from chair, facial expression, and speech are the most highly correlated to actual outcomes (respectively, r = 0.901, n = 8; r = 0.769, n = 10; r = 0.577, n = 21; r = 0.539, n = 14). For total UPDRS-III score predictions, there is not a strong linear correlation to actual outcomes (r = 0.110, n = 39) and the average percent error between actual and predicted outcome is 93%.

Table 3 displays the same information for predictions involving the left side. The strongest linear relationships observed come from predictions concerning ipsilateral motor outcome (left hand movements, r = 0.607, n = 61; left-handed finger taps, r = 0.533, n = 65; left upper extremity posture, r = 0.491, n = 63; left-handed rapid alternating movements, r = 0.436, n = 51). Predictions of total UPDRS-III outcome do not strongly correlate to actual outcome (r = 0.249, n =115) and are 70% less than actual outcome.

Statistical maps for selected subscores are shown in Figures 7-18, along with visualizations of subscore-specific probabilistic manifolds. In the top panel of Figure 7, the statistical map of left upper extremity tremor outcome demonstrates that stimulation applied to the dorsomedial, dorsolateral, and anterior regions of the right STN corresponds to a decline in the outcome measure, while ventral stimulation corresponds to improvement. In the bottom panel, it is clear that the manifold captures both the detrimental effects of dorsomedial, dorsolateral, and anterior stimulation, as well as the adjuvant effects of ventral stimulation.

In Figure 8, the statistical map suggests benefits of left STN-DBS on right upper extremity tremor outcome regardless of stimulation location, although dorsal stimulation is associated with the greatest improvement. However, it is

noteworthy that the probabilistic manifold reveals a region in the posterior, inferior aspect of the left STN which may predispose to decline when the therapeutic VTA falls within its boundaries.

Figures 9 and 10 show statistical maps and probabilistic manifolds for leg agility outcomes in right-side and left-side subjects, respectively. The outcome for right STN stimulation is negatively impacted by dorsally and anteriorly-directed stimulation, and the manifold learns a relatively well-defined region of space to be avoided. Interestingly, the outcome for left STN stimulation tends to decline with dorsal stimulation as well as posterior, ventral stimulation, and the probabilistic manifold successfully captures the necessity of avoiding each distinct regions.

As can be seen in Figures 11 and 12, body bradykinesia and hypokinesia outcome is generally improved following stimulation anywhere within or around the STN, with little difference between right and left implantations. The right and left-sided statistical maps for this outcome suggest a detriment following ventral stimulation, although this effect is not strong enough to appear in the predictions of the probabilistic manifold of either the right or left side.

The statistical map and probabilistic manifold for gait outcome following right STN-DBS is shown in Figure 13. Stimulation in most regions leads to improvement, especially when directed ventrally, although a limited location dorsal to the STN is associated with decline. For the left STN (Figure 14), ventral regions within the STN and locations dorsal to it actually correspond to improvement, and the manifold predicts decline will occur when stimulation reaches areas that correspond to improvement for the right STN.

From Figure 15, we see that stimulation at the dorsal tip of the STN, as well as at dorsal regions outside of the STN, leads to decline in speech performance. However, for the left STN (Figure 16), declines in speech outcome occurs when stimulation is applied to ventromedial areas.

Figures 17 and 18 display statistical maps and probabilistic manifolds for the UPDRS-III composite of all subscores, less those for muscles ipsilateral to the implanted STN. For right-side implantations, most areas correspond with improvement, although decline is likely with lateral and dorsomedial stimulation. On the left side, all regions but the posterior lateral region outside of the STN leads to improvement.

Table 1. Summary comparison of actual outcomes vs. model predictions for every subscore in UPDRS-III for each of 48 subjects.

implanted side	subject	observations	Pearson's r	avg. percent error
right	1	14	-0.575	46
right	7	15	0.891	35
right	16	37	0.981	-48
right	28	135	0.835	-69
right	42	49	0.937	-67
right	52	29	0.739	-140
right	66	17	0.997	-85
right	73	37	0.984	-27
right	83	18	0.980	-54
right	84	33	0.685	-41
right	87	50	0.938	-70
right	99	81	0.832	8
right	144	11	0.977	-53
right	146	17	0.992	-37
right	210	26	0.902	-52
left	4	138	0.916	-79
left	11	17	0.594	5
left	15	146	0.917	-38
left	26	99	0.902	-67
left	32	34	0.993	-78
left	41	45	0.887	-72
left	43	70	0.778	-42
left	45	16	0.531	-51
left	47	37	0.850	-39
left	48	10	-0.135	31
left	50	102	0.821	-74
left	54	80	0.956	-64
left	56	71	0.752	-34
left	57	67	0.936	-73
left	61	81	0.879	-76
left	63	36	0.983	-84
left	65	63	0.162	-9
left	67	104	0.834	-69
left	69	70	0.824	-63
left	72	90	0.857	-83
left	75	35	0.974	-78
left	82	53	0.886	-72
left	90	61	0.635	-33
left	105	25	0.498	-3
left	106	69	0.972	-42
left	117	35	0.329	-38
left	120	12	0.986	-87
left	129	11	0.063	4
left	132	65	0.795	-9
left	139	39	0.958	-69
left	156	44	0.829	-36
left	167	19	0.994	-80
left	191	18	0.997	-66

Table 2. Summary comparison of actual outcomes vs. model predictions for each subscore in UPDRS-III for right-implanted subjects. Ipsilateral motor outcome statistics are shown in faded text. (U.E.: upper extremity; L.E.: lower extremity)

UPDRS subscore	implanted side	observations	Pearson's r	avg. percent error
tremor at rest (face)	right	8	0.901	-40
rigidity (neck)	right	23	0.224	-41
speech	right	14	0.539	-30
facial expression	right	21	0.577	-44
body bradykinesia and hypokinesia	right	32	-0.102	-54
posture	right	23	0.485	-15
postural stability	right	18	0.238	36
gait	right	27	0.361	-31
arising from chair	right	10	0.769	0
tremor at rest (right U.E.)	right	21	0.239	-51
rigidity (right U.E.)	right	29	0.218	-41
rapid alternating (right U.E.)	right	24	0.162	-23
action postural (right U.E.)	right	15	0.381	-13
hand movements (right U.E.)	right	17	-0.036	-44
finger taps (right U.E.)	right	24	0.004	-41
tremor at rest (right L.E.)	right	18	-0.140	-29
rigidity (right L.E.)	right	28	-0.269	-57
leg agility (right L.E.)	right	22	0.503	3
tremor at rest (left U.E.)	right	22	0.334	-37
rigidity (left U.E.)	right	32	0.191	-57
rapid alternating (left U.E.)	right	28	0.333	-60
action postural (left U.E.)	right	19	0.295	-41
hand movements (left U.E.)	right	31	-0.335	-65
finger taps (left U.E.)	right	35	-0.043	-62
tremor at rest (left L.E.)	right	18	0.493	-36
rigidity (left L.E.)	right	30	-0.189	-58
leg agility (left L.E.)	right	22	0.312	-7
UPDRS-III total	right	39	0.110	-93

Table 3. Summary comparison of actual outcomes vs. model predictions for each subscore in UPDRS-III for right-implanted subjects. Ipsilateral motor outcome statistics are shown in faded text. (U.E.: upper extremity; L.E.: lower extremity)

UPDRS subscore	implanted side	observations	Pearson's r	avg. percent error
tremor at rest (face)	left	44	0.361	-34
rigidity (neck)	left	78	-0.048	-44
speech	left	52	0.307	-33
facial expression	left	69	0.207	-48
body bradykinesia and hypokinesia	left	97	0.065	-63
posture	left	58	0.381	-18
postural stability	left	64	0.100	-33
gait	left	57	0.192	-31
arising from chair	left	50	0.345	-40
tremor at rest (right U.E.)	left	95	0.092	-57
rigidity (right U.E.)	left	110	0.148	-62
rapid alternating (right U.E.)	left	83	0.107	-57
action postural (right U.E.)	left	104	0.050	-66
hand movements (right U.E.)	left	85	0.150	-60
finger taps (right U.E.)	left	97	0.066	-60
tremor at rest (right L.E.)	left	88	0.254	-62
rigidity (right L.E.)	left	90	0.258	-57
leg agility (right L.E.)	left	79	0.377	-49
tremor at rest (left U.E.)	left	57	0.323	-6
rigidity (left U.E.)	left	65	0.221	-15
rapid alternating (left U.E.)	left	51	0.436	-21
action postural (left U.E.)	left	63	0.491	-22
hand movements (left U.E.)	left	61	0.607	-37
finger taps (left U.E.)	left	65	0.533	-36
tremor at rest (left L.E.)	left	45	0.125	-21
rigidity (left L.E.)	left	72	0.379	-41
leg agility (left L.E.)	left	63	0.404	4
UPDRS-III total	left	115	0.249	-70

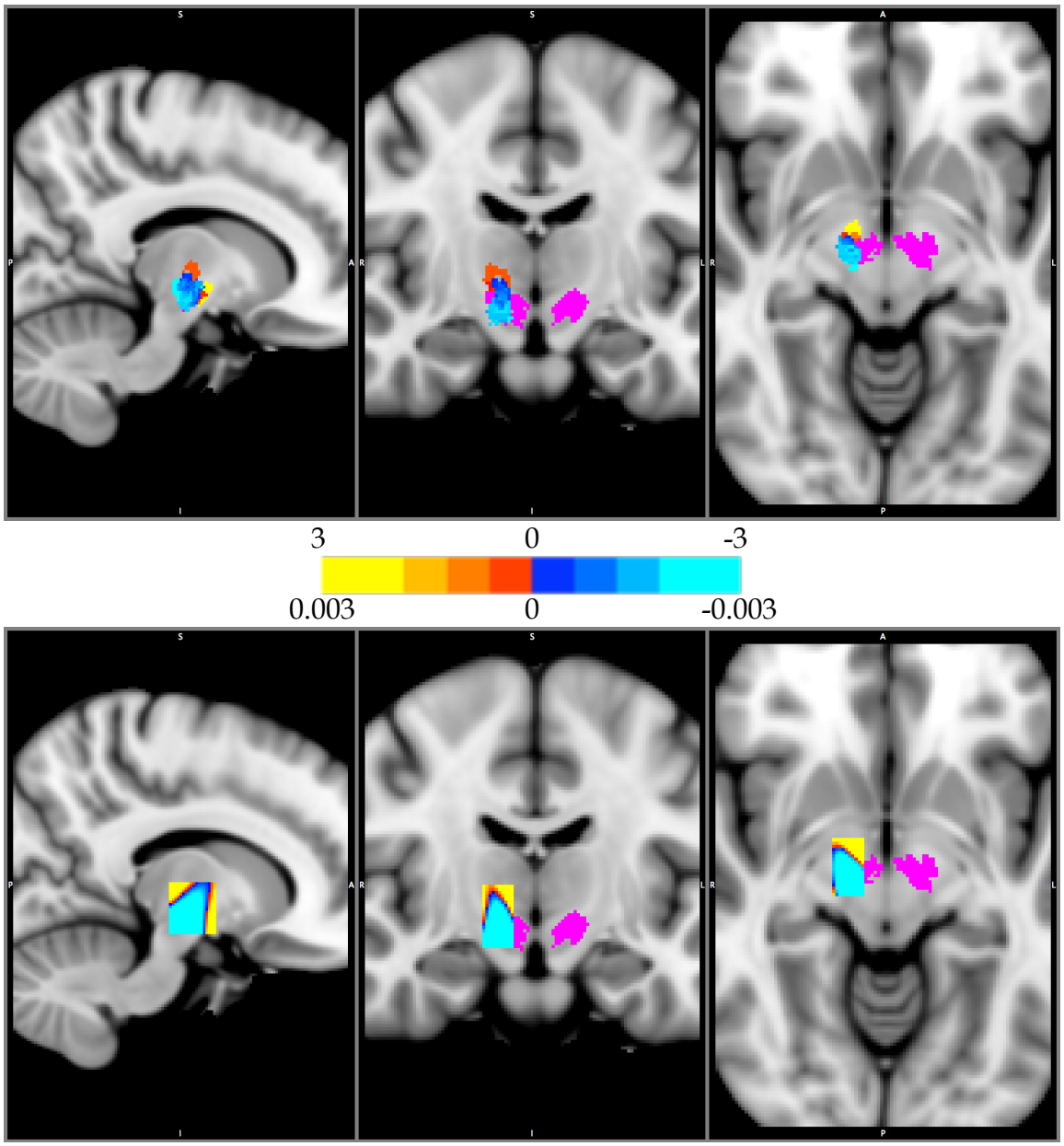

Figure 7. Top panel: Statistical map of left upper extremity tremor outcome for right-implanted subjects (radiological orientation). Bottom panel: Probabilistic manifold of left upper extremity tremor outcome for right-implanted subjects (radiological orientation).

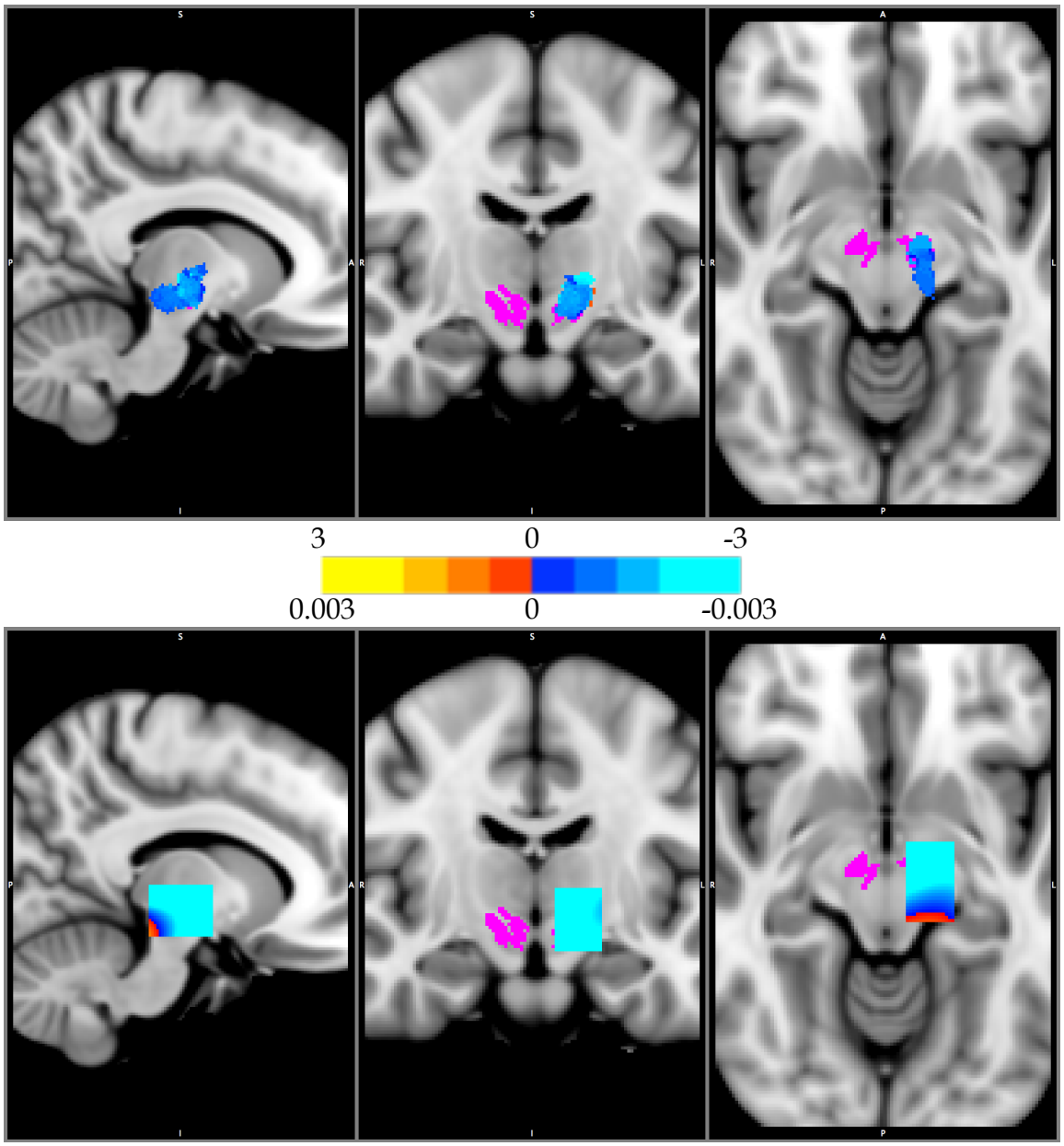

Figure 8. Top panel: Statistical map of right upper extremity tremor outcome for left-implanted subjects (radiological orientation). Bottom panel: Probabilistic manifold of right upper extremity tremor outcome for left-implanted subjects (radiological orientation).

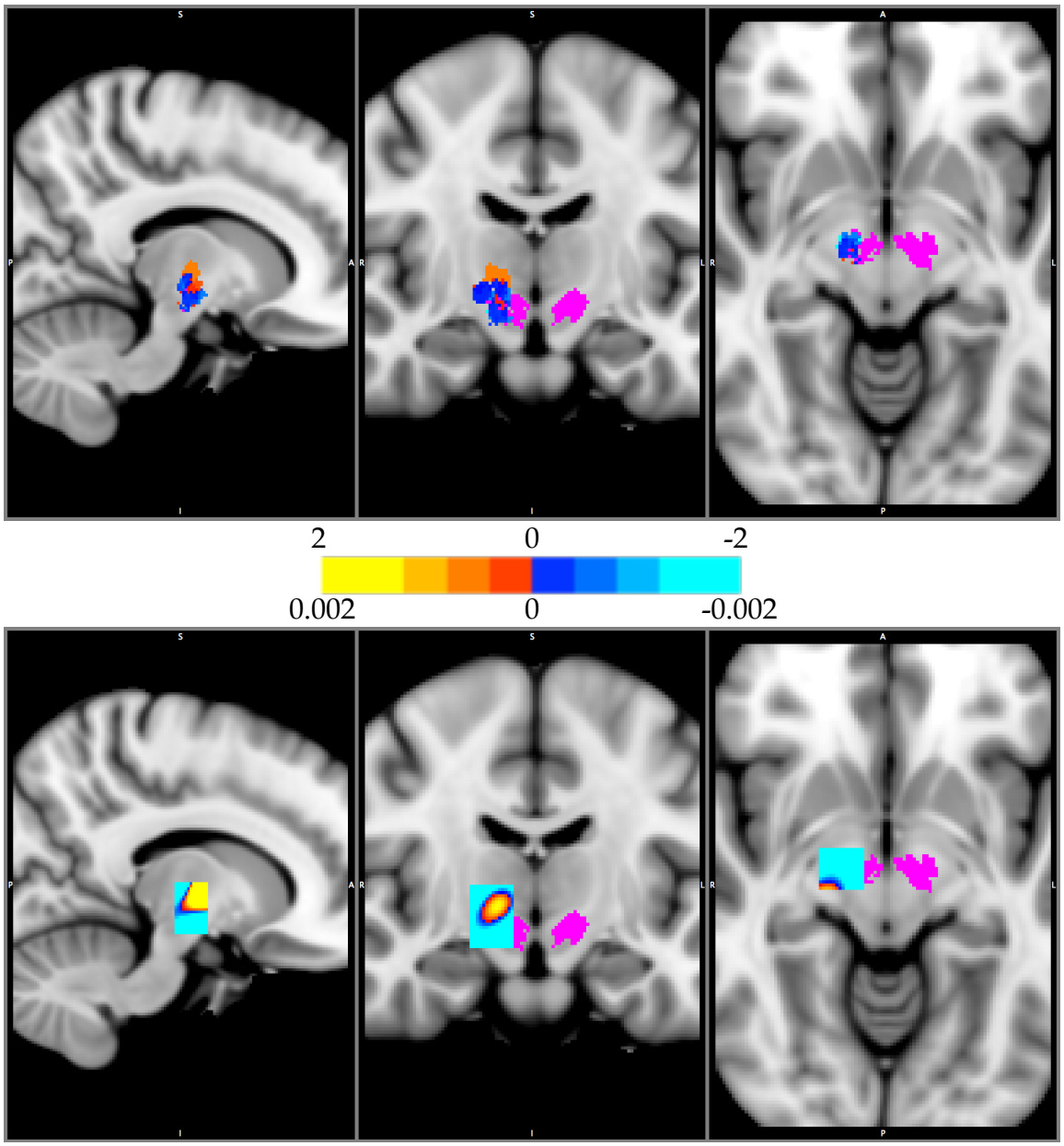

Figure 9. Top panel: Statistical map of left-leg agility outcome for right-implanted subjects (radiological orientation). Bottom panel: Probabilistic manifold of left-leg agility outcome for right-implanted subjects (radiological orientation).

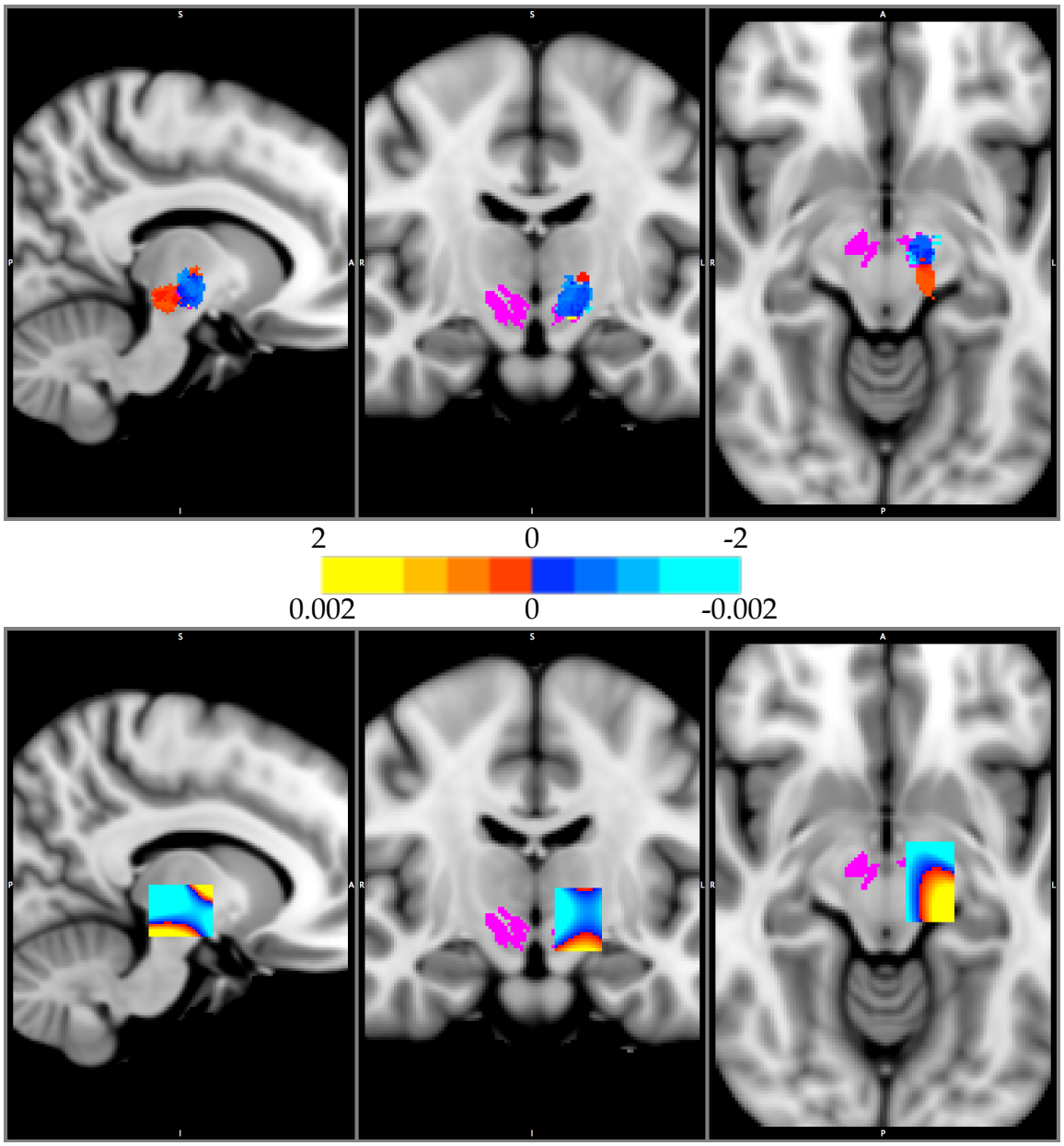

Figure 10. Top panel: Statistical map of right-leg agility outcome for left-implanted subjects (radiological orientation). Bottom panel: Probabilistic manifold of right-leg agility outcome for left-implanted subjects (radiological orientation).

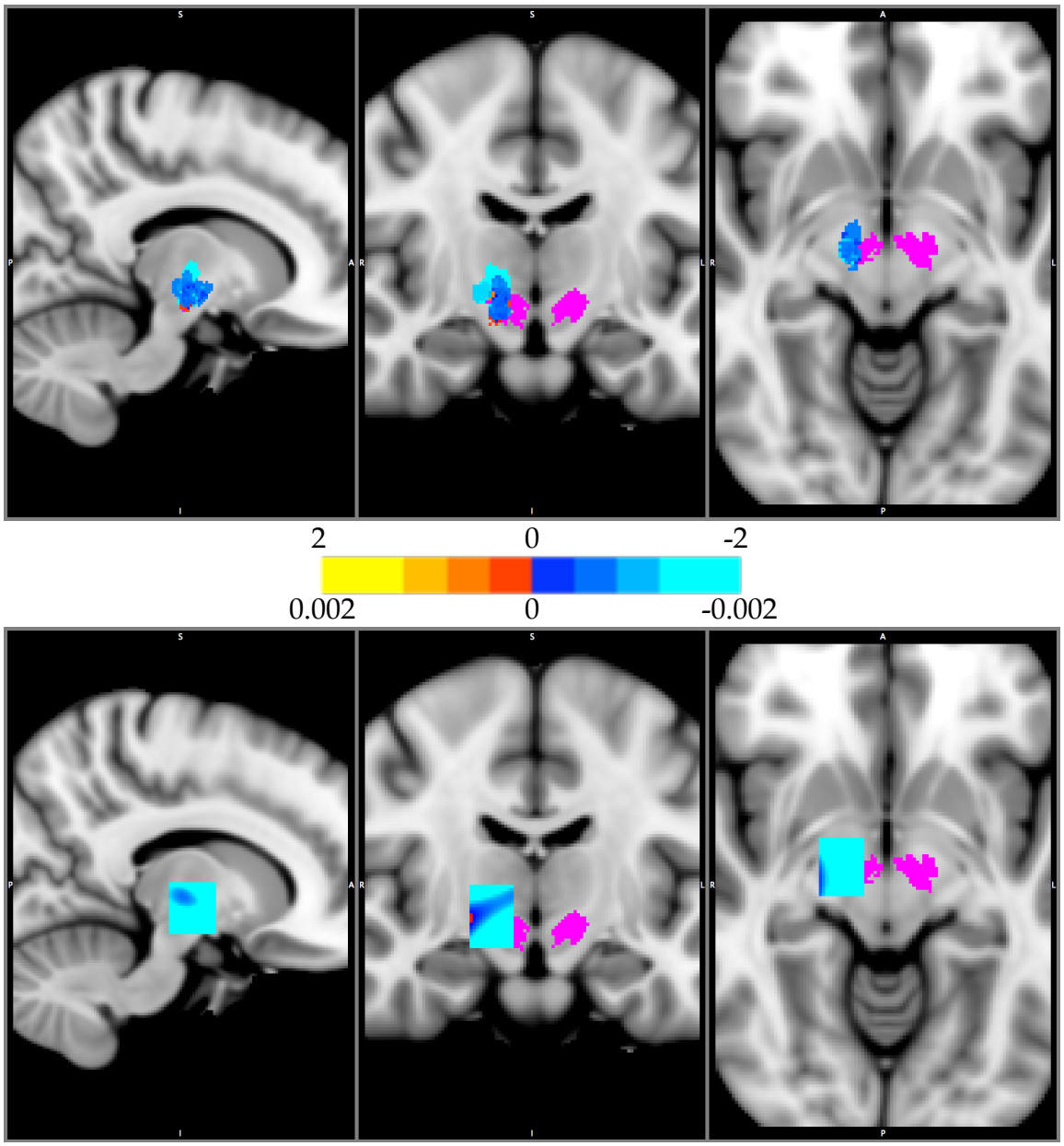

Figure 11. Top panel: Statistical map of body bradykinesia and hypokinesia outcome for right-implanted subjects (radiological orientation). Bottom panel: Probabilistic manifold of body bradykinesia and hypokinesia outcome for right-implanted subjects (radiological orientation).

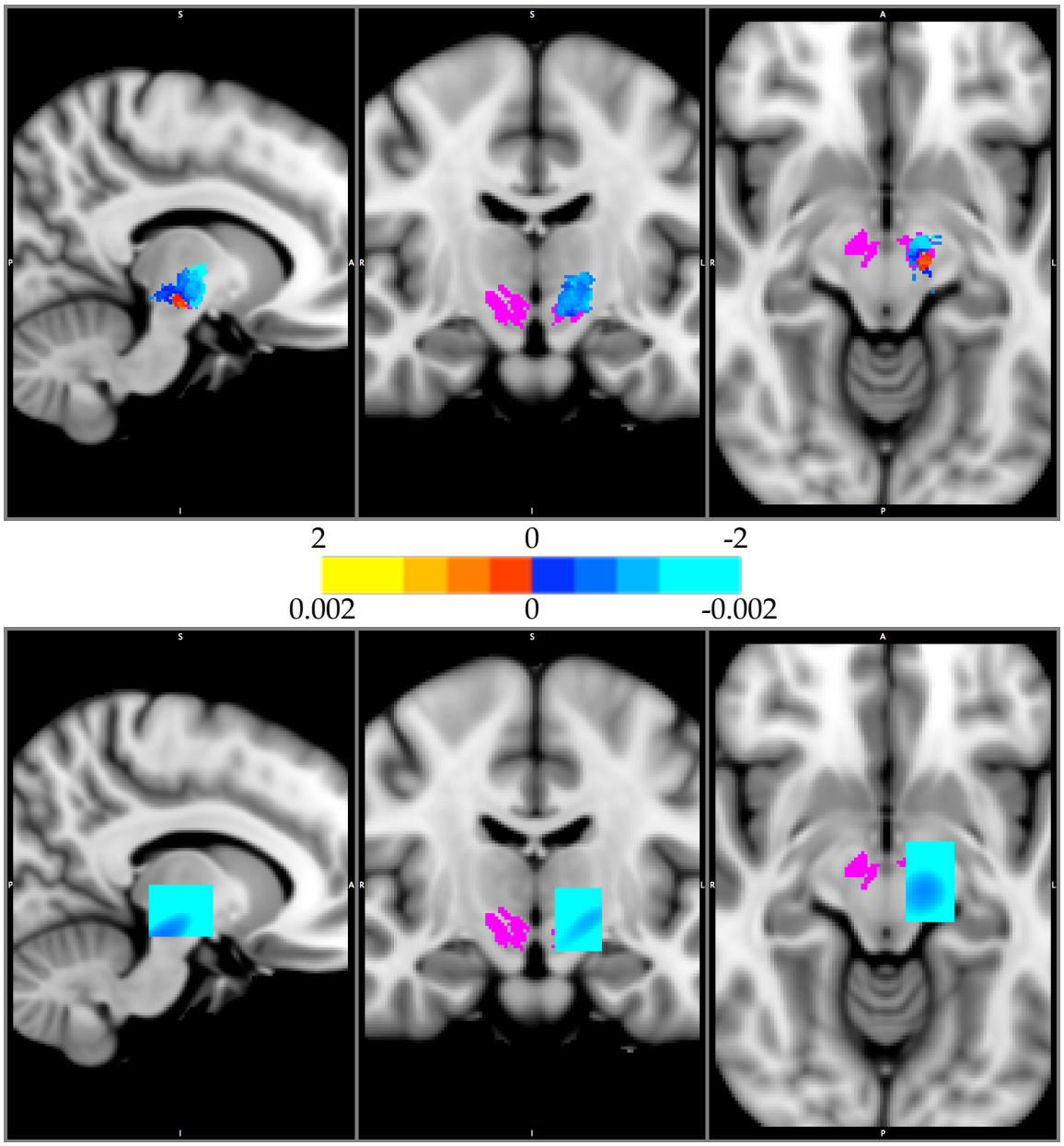

Figure 12. Top panel: Statistical map of body bradykinesia and hypokinesia outcome for left-implanted subjects (radiological orientation). Bottom panel: Probabilistic manifold of body bradykinesia and hypokinesia outcome for left-implanted subjects (radiological orientation).

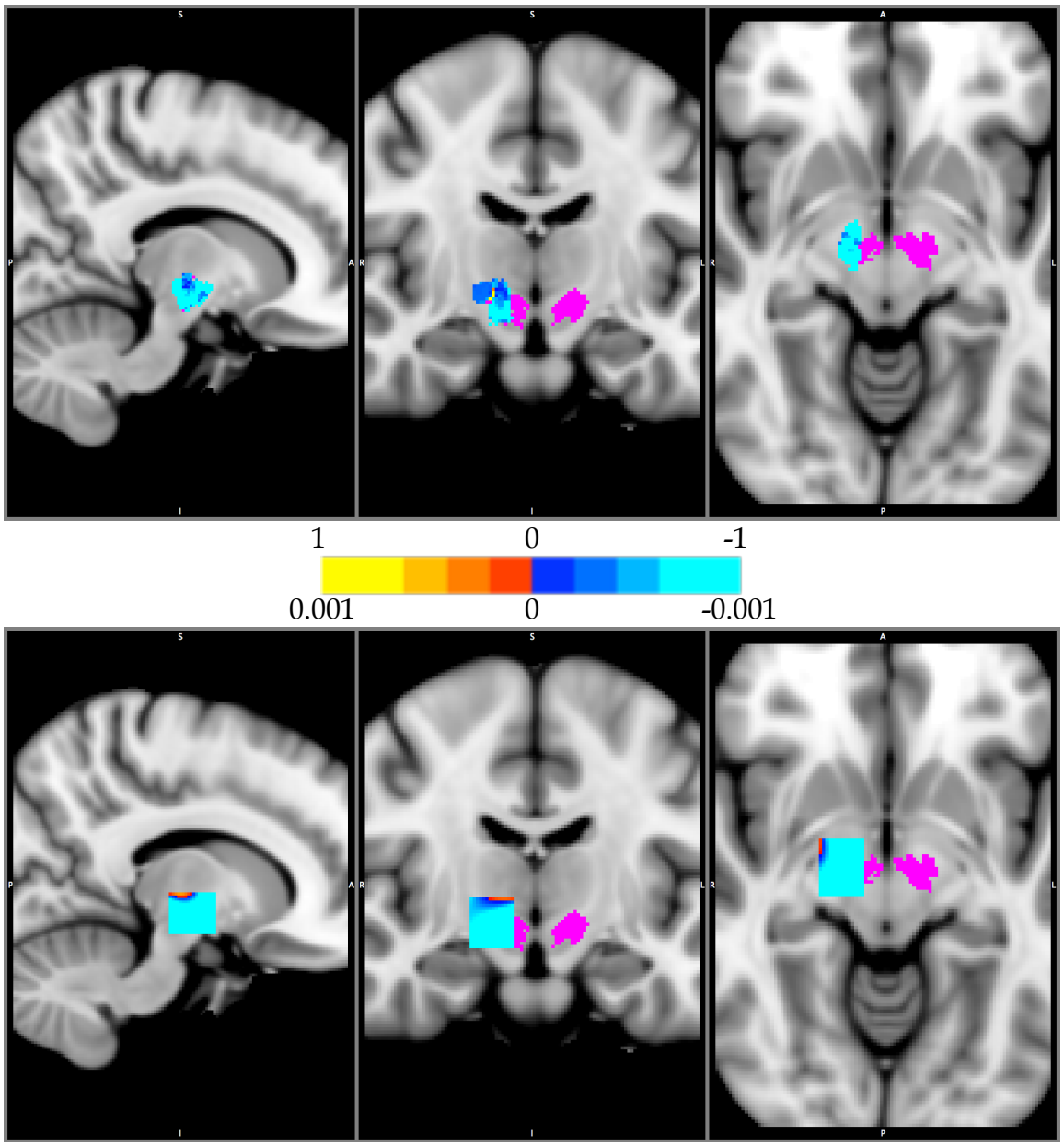

Figure 13. Top panel: Statistical map of gait outcome for right-implanted subjects (radiological orientation). Bottom panel: Probabilistic manifold of gait outcome for right-implanted subjects (radiological orientation).

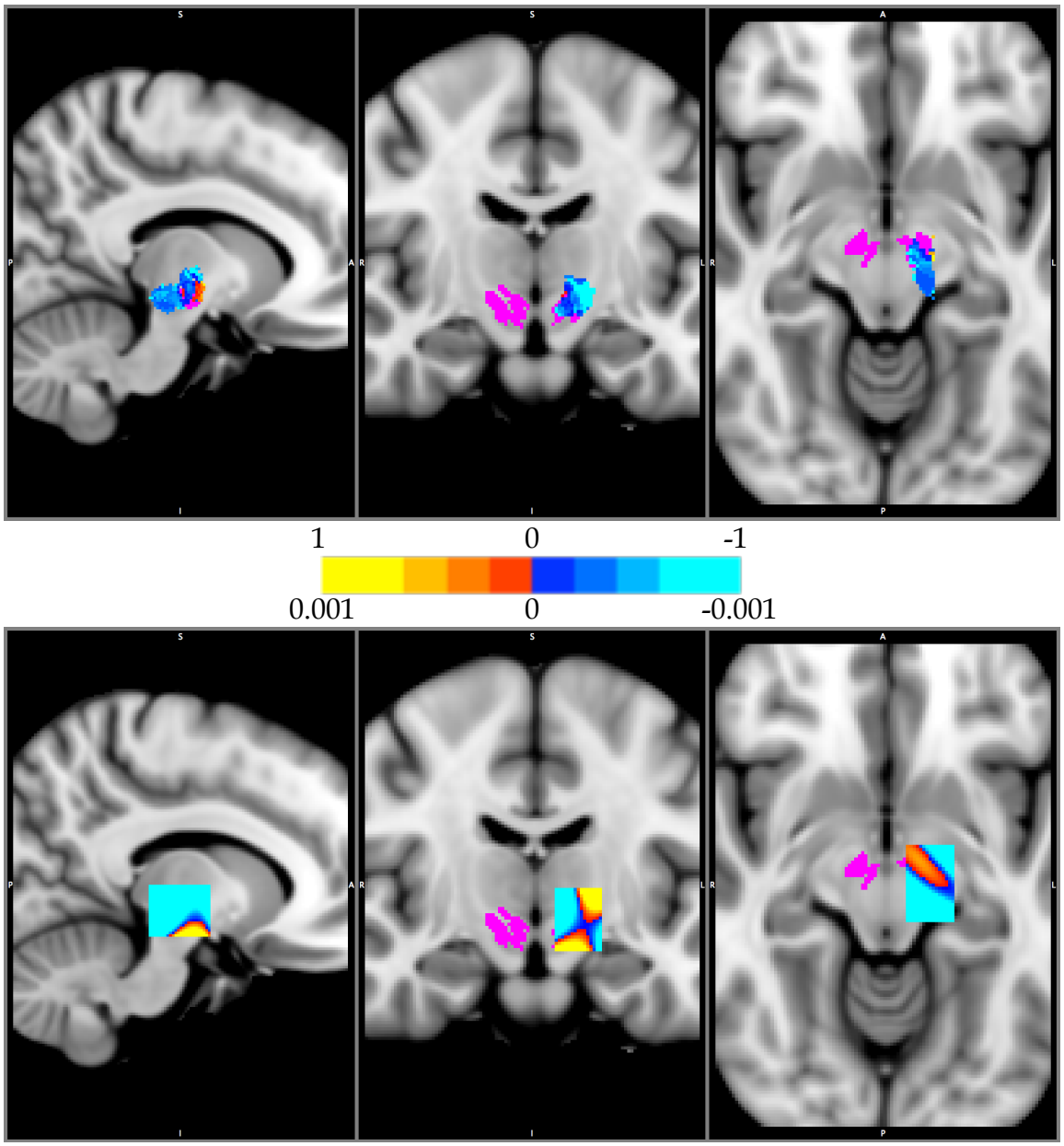

Figure 14. Top panel: Statistical map of gait outcome for left-implanted subjects (radiological orientation). Bottom panel: Probabilistic manifold of gait outcome for left-implanted subjects (radiological orientation).

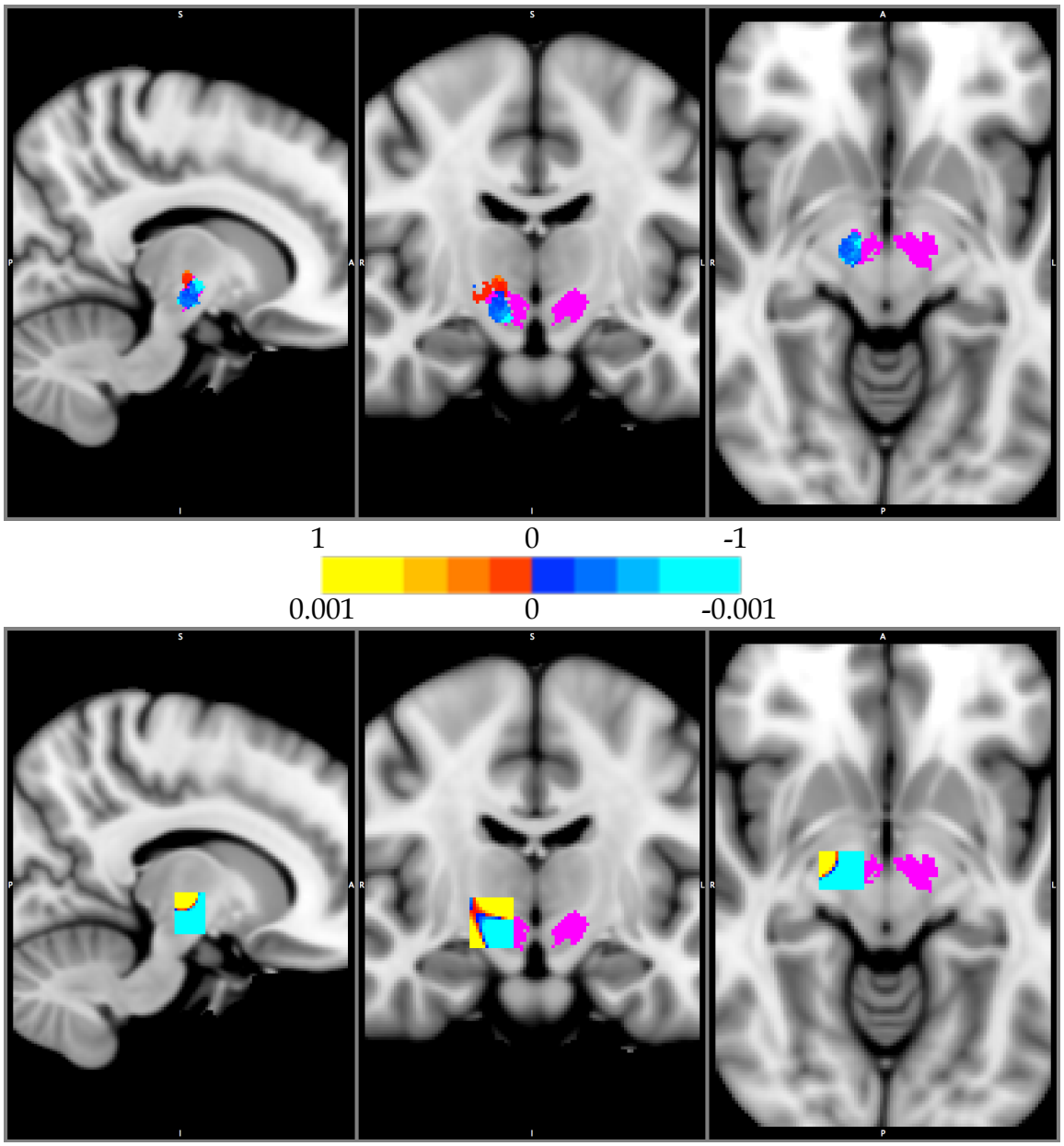

Figure 15. Top panel: Statistical map of speech outcome for right-implanted subjects (radiological orientation). Bottom panel: Probabilistic manifold of speech outcome for right-implanted subjects (radiological orientation).

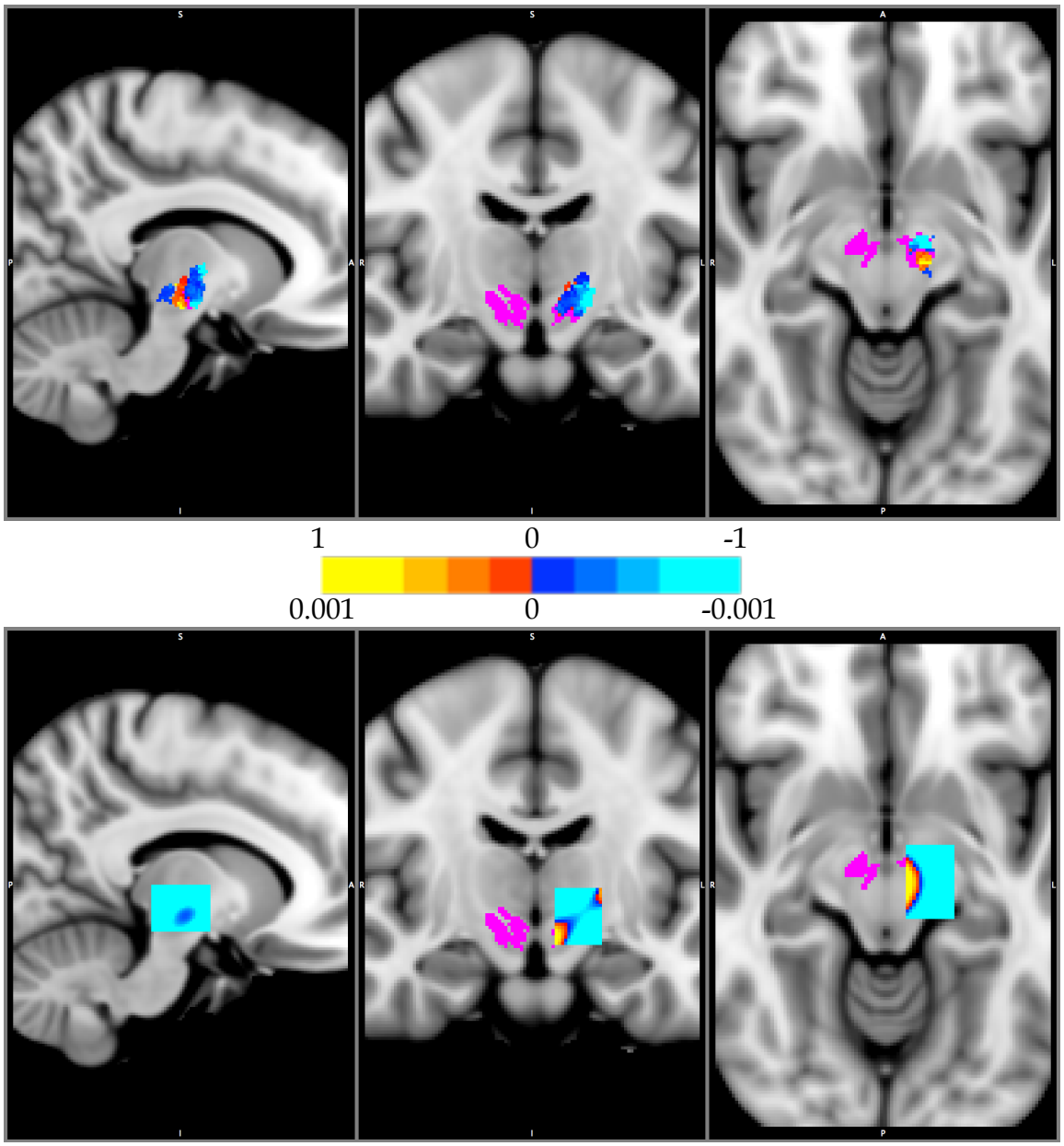

Figure 16. Top panel: Statistical map of speech outcome for left-implanted subjects (radiological orientation). Bottom panel: Probabilistic manifold of speech outcome for left-implanted subjects (radiological orientation).

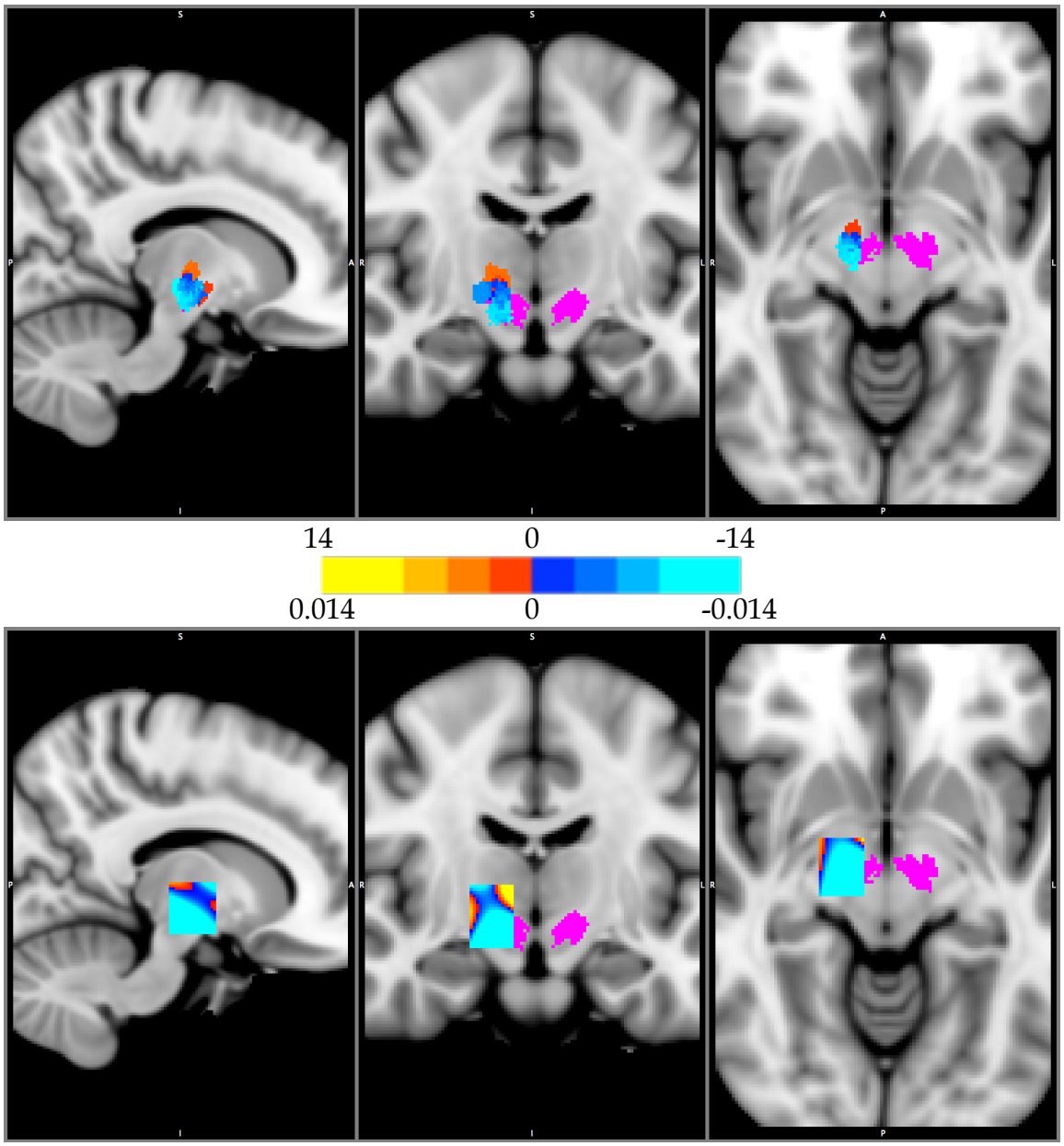

Figure 17. Top panel: Statistical map of left-side UPDRS-III outcome for right-implanted subjects (radiological orientation). Bottom panel: Probabilistic manifold of left-side UPDRS-III outcome for right-implanted subjects (radiological orientation).

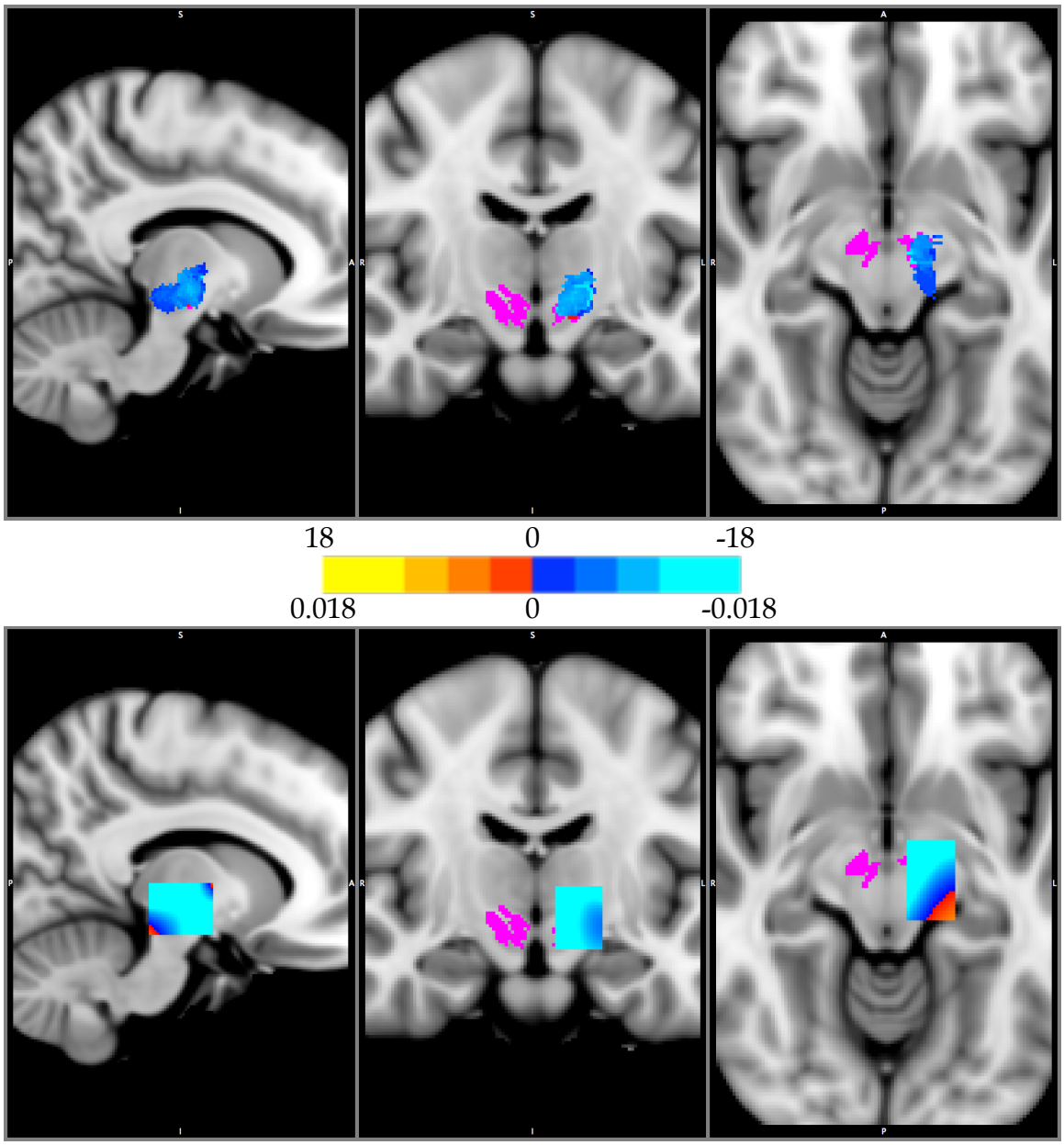

Figure 18. Top panel: Statistical map of right-side UPDRS-III outcome for left-implanted subjects (radiological orientation). Bottom panel: Probabilistic manifold of right-side UPDRS-III outcome for left-implanted subjects (radiological orientation).

DISCUSSION

The statistical analysis of the model's predictive ability qualitatively demonstrates its success for most subjects and most subscores. Failures at the subject level may be attributed to varying levels of success of the neuroimaging processing steps of the pipeline, which is currently left unquantified. Future iterations of the pipeline, therefore, should include model terms for the accuracy of standardization steps taken for each subject. Subscore-level failures, on the other hand, may reflect the fact that not all aspects of motor dysfunction in PD are amenable to treatment with DBS, or that some particular outcome is not predominantly determined by stimulation at specific locations in and around the STN.

Previous studies suggest that stimulation anywhere in the vicinity of the STN may lead to motor improvement as assessed by UPDRS-III (Kasasbeh et al., 2013; Eisenstein et al., 2014). By and large, this finding is replicated here and can be explained by the fact that there is anatomical overlap between functionally segregated subregions of the STN (Alkemade et al., 2015).

It is crucial to note, however, that this analysis is the first that we know of to examine each subscore of UPDRS-III for the effects of location-specific stimulation, and as such, validation of the model's predictions is incomplete. In this respect, prospective comparison of actual and predicted outcomes, ideally from subjects whose previous data do not inform the creation of the model, would provide a useful evaluation.

The estimation of VTAs in the pipeline is rudimentary, but highly amenable to computation. In future studies with more advanced computational tools, we could model tissue activation separately for cell bodies and fiber tracts, which will provide exceptionally greater accuracy in determining the spread of electrical stimulation.

Further development of the pipeline described must include a cross-validation step, wherein each term of the GLM is evaluated for predictive utility. Given that each term in the presented model relates solely to anatomical location, it is essential to include other terms in the cross-validation, such as subject age, length of time since surgery, and the success of neuroimaging processing.

Upon validation of the probabilistic manifolds for individual UPDRS-III subscores, multiple subscores may be modeled simultaneously to create a tool that is useful to the clinician caring for a PD patient whose chief complaints revolve around multiple symptoms. If such an approach is supported through further validation studies, it may improve the ability to personalize DBS therapy to the symptoms of a particular patient.

Finally, recent advances in neuroimaging, DBS electrode design, and functional neurosurgical techniques will allow for ever more minute control of therapeutic stimulation. To help such progress translate to the increased efficacy of STN-DBS in PD, approaches such as that described will be required.

REFERENCES

Hirtz D, Thurman DJ, Gwinn-Hardy K, Mohamed M, Chaudhuri AR, Zalutsky R. How common are the "common" neurologic disorders? Neurology. 2007;68:326–37.

Wirdefeldt K, Adami HO, Cole P, Trichopoulos D, Mandel J. Epidemiology and etiology of Parkinson's disease: a review of the evidence. Eur J Epidemiol. 2011 Jun;26 Suppl 1:S1-58.

Fahn S, Elton R, Members of the updrs Development Committee. In: Fahn S, Marsden CD, Calne DB, Goldstein M, eds. Recent Developments in Parkinson's Disease, Vol 2. Florham Park, NJ. Macmillan Health Care Information 1987, pp 153-163, 293-304.

Stocchi F, Tagliati M, Olanow CW. Treatment of levodopa-induced motor complications. Mov Disord 2008;23(Suppl. 3):S599e612.

Bronstein JM, Tagliati M, Alterman RL, Lozano AM, Volkmann J, Stefani A, Horak FB, Okun MS, Foote KD, Krack P, Pahwa R, Henderson JM, Hariz MI, Bakay RA, Rezai A, Marks WJ Jr, Moro E, Vitek JL, Weaver FM, Gross RE, DeLong MR. Deep brain stimulation for Parkinson disease: an expert consensus and review of key issues. Arch Neurol. 2011 Feb;68(2):165.

Bergman H, Wichmann T, DeLong MR. Reversal of experimental parkinsonism by lesions of the subthalamic nucleus. Science. 1990;249(4975):1436-1438. 2.

DeLong MR. Primate models of movement disorders o fbasal ganglia origin. Trends Neurosci. 1990;13(7):281-285.

Aziz TZ, Peggs D, Sambrook MA, Crossman AR. Lesion of the subthalamic nucleus for the alleviation of 1-methyl-4-phenyl-1,2,3,6-tetrahydropyridine (MPTP)-induced parkinsonism in the primate. Mov Disord. 1991;6(4):288-292.

Okun MS, Tagliati M, Pourfar M, Fernandez HH, Rodriguez RL, Alterman RL, Foote KD. Management of referred deep brain stimulation failures: a retrospective analysis from 2 movement disorders centers. Arch Neurol. 2005 Aug;62(8):1250-5.

Schüpbach WM, Maltête D, Houeto JL, du Montcel ST, Mallet L, Welter ML, Gargiulo M, Béhar C, Bonnet AM, Czernecki V, Pidoux B, Navarro S, Dormont D, Cornu P, Agid Y. Neurosurgery at an earlier stage of Parkinson disease: a randomized, controlled trial. Neurology. 2007 Jan 23;68(4):267-71.

Merola A, Romagnolo A, Bernardini A, Rizzi L, Artusi CA, Lanotte M, Rizzone MG, Zibetti M, Lopiano L. Earlier versus later subthalamic deep brain stimulation in Parkinson's disease. Parkinsonism Relat Disord. 2015 Jun 4. pii: S1353-8020(15)00244-8.

Charles PD, Van Blercom N, Krack P, et al. Predictors of effective bilateral subthalamic nucleus stimulation for PD. Neurology. 2002;59(6):932-934.

Kleiner-Fisman G, Herzog J, Fisman DN, et al. Subthalamic nucleus deep brain stimulation: summary and meta-analysis of outcomes. Mov Disord. 2006;21 (suppl 14):S290-S304.

Weaver FM, Follett K, Stern M, Hur K, Harris C, Marks WJ Jr, Rothlind J, Sagher O, Reda D, Moy CS, Pahwa R, Burchiel K, Hogarth P, Lai EC, Duda JE, Holloway K, Samii A, Horn S, Bronstein J, Stoner G, Heemskerk J, Huang GD; CSP 468 Study Group. Bilateral deep brain stimulation vs best medical therapy for patients with advanced Parkinson disease: a randomized controlled trial. JAMA. 2009 Jan 7;301(1):63-73.

Blomstedt P, Hariz MI. Hardware-related complications of deep brain stimulation: a ten year experience. Acta Neurochir (Wien). 2005 Oct;147(10):1061-4; discussion 1064.

Videnovic A, Metman LV. Deep brain stimulation for Parkinson's disease: prevalence of adverse events and need for standardized reporting. Mov Disord. 2008 Feb 15;23(3):343-9.

Hamani C, Lozano AM. Hardware-related complications of deep brain stimulation: a review of the published literature. Stereotact Funct Neurosurg. 2006;84(5-6):248-51.

Deuschl G, Schade-Brittinger C, Krack P, Volkmann J, Schäfer H, Bötzel K, Daniels C, Deutschländer A, Dillmann U, Eisner W, Gruber D, Hamel W, Herzog J, Hilker R, Klebe S, Kloss M, Koy J, Krause M, Kupsch A, Lorenz D, Lorenzl S, Mehdorn HM, Moringlane JR, Oertel W, Pinsker MO, Reichmann H, Reuss A, Schneider GH, Schnitzler A, Steude U, Sturm V, Timmermann L, Tronnier V, Trottenberg T, Wojtecki L, Wolf E, Poewe W, Voges J; German Parkinson Study Group, Neurostimulation Section. A randomized trial of deep-brain stimulation for Parkinson's disease. N Engl J Med. 2006 Aug 31;355(9):896-908. Erratum in: N Engl J Med. 2006 Sep 21;355(12):1289.

Rezai AR, Machado AG, Deogaonkar M, Azmi H, Kubu C, Boulis NM. Surgery for movement disorders. Neurosurgery. 2008 Feb;62 Suppl 2:809-38; discussion 838-9.

Machado A, Rezai AR, Kopell BH, Gross RE, Sharan AD, Benabid AL. Deep brain stimulation for Parkinson's disease: surgical technique and perioperative management. Mov Disord. 2006 Jun;21 Suppl 14:S247-58.

Malone DA Jr, Dougherty DD, Rezai AR, Carpenter LL, Friehs GM, Eskandar EN, Rauch SL, Rasmussen SA, Machado AG, Kubu CS, Tyrka AR, Price LH, Stypulkowski PH, Giftakis JE, Rise MT, Malloy PF, Salloway SP, Greenberg BD. Deep brain stimulation of the ventral capsule/ventral striatum for treatment-resistant depression. Biol Psychiatry. 2009 Feb 15;65(4):267-75.

Voon V, Kubu C, Krack P, Houeto JL, Troster AI (2006) Deep brain stimulation: Neuropsychological and neuropsychiatric issues. Mov. Disord. 21(Suppl. 14): S305–S327.

Parsons TD, Rogers SA, Braaten AJ, Woods SP, Troster AI (2006) Cognitive sequelae of subthalamic nucleus deep brain stimulation in Parkinson's disease: a meta-analysis. Lancet Neurol. 5:578–588.

Temel Y, Kessels A, Tan S, Topdag A, Boon P, Visser-Vandewalle V (2006) Behavioural changes after bilateral subthalamic stimulation in advanced Parkinson disease: A systematic review. Parkinsonism Relat. Disord. 12:265–272.

Obeso I, Wilkinson L, Casabona E, Bringas ML, Alvarez M, Alvarez L, Pavon N, Rodriguez-Oroz MC, Macias R, Obeso JA, Jahanshahi M (2011) Deficits in inhibitory control and conflict resolution on cognitive and motor tasks in Parkinson's disease. Exp. Brain Res. 212:371–384.

Jahanshahi M, Ardouin CM, Brown RG, Rothwell JC, Obeso J, Albanese A, Rodriguez-Oroz MC, Moro E, Benabid AL, Pollak P, Limousin-Dowsey P (2000) The impact of deep brain stimulation on executive function in Parkinson's disease. Brain 123(6):1142–1154.

Witt K, Pulkowski U, Herzog J, Lorenz D, Hamel W, Deuschl G, Krack P (2004) Deep brain stimulation of the subthalamic nucleus improves cognitive flexibility but impairs response inhibition in Parkinson disease. Arch. Neurol. 61:697–700.

Witt K, Krack P, Deuschl G (2006) Change in artistic expression related to subthalamic stimulation. J. Neurol. 253:955–956.

Witt K, Granert O, Daniels C, Volkmann J, Falk D, van Eimeren T, Deuschl G (2013) Cognitive outcomes after STN-DBS in Parkinson's disease. Brain 136:2109–2119

Schroeder U, Kuehler A, Haslinger B, Erhard P, Fogel W, Tronnier VM, Lange KW, Boecker H, Ceballos-Baumann AO (2002) Subthalamic nucleus stimulation affects striato-anterior cingulate cortex circuit in a response conflict task: a PET study. Brain 125:1995–2004.

Brittain JS, Watkins KE, Joundi RA, Ray NJ, Holland P, Green AL, Aziz TZ, Jenkinson N (2012) A role for the subthalamic nucleus in response inhibition during conflict. J. Neurosci. 32:13396–13401.

Rizzone M, Lanotte M, Bergamasco B, Tavella A, Torre E, Faccani G, Melcarne A, Lopiano L. Deep brain stimulation of the subthalamic nucleus in Parkinson's disease: effects of variation in stimulation parameters. J Neurol Neurosurg Psychiatry 2001;71:215–9.

Moro E, Esselink RJ, Xie J, Hommel M, Benabid AL, Pollak P. The impact on Parkinson's disease of electrical parameter settings in STN stimulation. Neurology 2002;59:706–13.

Volkmann J, Herzog J, Kopper F, Deuschl G. Introduction to the programming of deep brain stimulators. Mov Disord 2002;17(Suppl 3):181–7.

O'Suilleabhain PE, Frawley W, Giller C, Dewey RB. Tremor response to polarity, voltage, pulse width and frequency of thalamic stimulation. Neurology 2003;60:786–90.

Volkmann J, Daniels C, Witt K. Neuropsychiatric effects of subthalamic neurostimulation in Parkinson disease. Nat Rev Neurol. 2010 Sep;6(9):487-98.

Da Cunha C, Boschen SL, Gómez-A A, Ross EK, Gibson WS, Min HK, Lee KH, Blaha CD. Toward sophisticated basal ganglia neuromodulation: Review on basal ganglia deep brain stimulation. Neurosci Biobehav Rev. 2015 Feb 12. pii: S014-7634(15)00048-2.

Bolam, J.P., Hanley, J.J., Booth, P.A.C., Bevan, M.D., 2000. Synaptic organisation of the basal ganglia. J. Anat. 196, 527–542.

Nambu, A., Tokuno, H., Hamada, I., Kita, H., Imanishi, M., Akazawa, T., Ikeuchi, Y., Hasegawa, N., 2000. Excitatory cortical inputs to pallidal neurons via the subthalamic nucleus in the monkey. J. Neurophysiol. 84, 289–300.

Miwa, H., Fuwa, T., Nishi, K., Kondo, T., 2001. Subthalamo-pallido-striatal axis: a feedback system in the basal ganglia. Neuroreport 12, 3795–3798.

Jaeger, D., Kita, H., 2011. Functional connectivity and integrative properties of globus pallidus neurons. Neuroscience 198, 44–53.

Obeso, J.A., Guridi, J., Nambu, A., Crossman, A.R., 2013. Motor manifestations and basal ganglia output activity: the paradox continues. Mov. Disord. 28, 416–418.

Surmeier, D.J., 2013. To go or not to go. Nature 494, 178–179.

Ullsperger, M., Danielmeier, C., Jocham, G., 2014. Neurophysiology of performance monitoring and adaptive behavior. Physiol. Rev. 94, 35–79.

Woolley, S.C., Rajan, R., Joshua, M., Doupe, A.J., 2014. Emergence of context-dependent variability across a basal ganglia network. Neuron 82, 208–223.

Wiecki TV, Frank MJ. A computational model of inhibitory control in frontal cortex and basal ganglia. Psychol Rev. 2013 Apr;120(2):329-55.

Jahanshahi M. Effects of deep brain stimulation of the subthalamic nucleus on inhibitory and executive control over prepotent responses in Parkinson's disease. Front Syst Neurosci. 2013 Dec 25;7:118.

Frank MJ. Hold your horses: a dynamic computational role for the subthalamic nucleus in decision making. Neural Netw. 2006 Oct;19(8):1120-36.

Afsharpour S. Topographical projections of the cerebral cortex to the subthalamic nucleus. J Comp Neurol. 1985 Jun 1;236(1):14-28.

Monakow KH, Akert K, Künzle H. Projections of the precentral motor cortex and other cortical areas of the frontal lobe to the subthalamic nucleus in the monkey. Exp Brain Res. 1978 Nov 15;33(3-4):395-403.

Yelnik J, Percheron G. Subthalamic neurons in primates: a quantitative and comparative analysis. Neuroscience. 1979;4(11):1717-43.

Coyne T, Silburn P, Cook R, Silberstein P, Mellick G, Sinclair F, Fracchia G, Wasson D, Stanwell P. Rapid subthalamic nucleus deep brain stimulation lead placement utilising CT/MRI fusion, microelectrode recording and test stimulation. Acta Neurochir Suppl. 2006;99:49-50.

Alexander GE, Crutcher MD, DeLong MR. Basal ganglia-thalamocortical circuits: parallel substrates for motor, oculomotor, prefrontal" and "limbic" functions. Prog Brain Res. 1990;85:119-46.

Joel D, Weiner I. The connections of the primate subthalamic nucleus: indirect pathways and the open-interconnected scheme of basal ganglia-thalamocortical circuitry. Brain Res Brain Res Rev. 1997 Feb;23(1-2):62-78. Review.

Karachi C, Yelnik J, Tandé D, Tremblay L, Hirsch EC, François C. The pallidosubthalamic projection: an anatomical substrate for nonmotor functions of the subthalamic nucleus in primates. Mov Disord. 2005 Feb;20(2):172-80.

Parent A, Hazrati LN. Functional anatomy of the basal ganglia. II. The place of subthalamic nucleus and external pallidum in basal ganglia circuitry. Brain Res Brain Res Rev. 1995 Jan;20(1):128-54. Review.

Temel Y, Blokland A, Steinbusch HW, Visser-Vandewalle V. The functional role of the subthalamic nucleus in cognitive and limbic circuits. Prog Neurobiol. 2005 Aug;76(6):393-413. Epub 2005 Oct 24. Review.

Bevan MD, Atherton JF, and Baufreton J. (2006). Cellular principles underlying normal and pathological activity in the subthalamic nucleus. Curr. Opin. Neurobiol. 16, 621–628.

Romanelli P, Esposito V, Schaal DW, Heit G. Somatotopy in the basal ganglia: experimental and clinical evidence for segregated sensorimotor channels. Brain Res. Brain Res. Rev. 2005;48(1):112–128.

Scheeringa R, Fries P, Petersson KM, Oostenveld R, Grothe I, Norris DG, Hagoort P, Bastiaansen MC. Neuronal dynamics underlying high- and low-frequency EEG oscillations contribute independently to the human BOLD signal. Neuron. 2011 Feb 10;69(3):572-83.

Manning JR, Jacobs J, Fried I, Kahana MJ (2009) Broadband shifts in local field po- tential power spectra are correlated with single-neuron spiking in humans. J Neurosci 29(43):13613–13620.

Dubois B, Boller F, Pillon B, Agid Y. (1991) Cognitive deficits in Parkinson's disease. In: Handbook of Neuropsychology, Vol. 5, (Eds F Boller and J Grafman), pp. 195–240. Elsevier, Amsterdam.

Willingham DB. (1998) A neuropsychological theory of motor skill learning. Psychological Review, 105, 558–584.

de Hemptinne C, Ryapolova-Webb ES, Air EL, Garcia PA, Miller KJ, Ojemann JG, Ostrem JL, Galifianakis NB, Starr PA. Exaggerated phase-amplitude coupling in the primary motor cortex in Parkinson disease. Proc Natl Acad Sci U S A. 2013 Mar 19;110(12):4780-5.

Young A, Penney J. (1993) Biochemical and functional organization of the basal ganglia. In J.Jankovic, & E. Tolosa (Eds.),Parkinson's disease and movement disorders, (pp. 1- 11). Baltimore: Williams and Wilkins.

Hammond C, Bergman H, Brown P (2007) Pathological synchronization in Parkinson's disease: Networks, models and treatments. Trends Neurosci 30(7):357–364.

Levy R, Hutchison WD, Lozano AM, Dostrovsky JO (2000) High-frequency synchroni- zation of neuronal activity in the subthalamic nucleus of parkinsonian patients with limb tremor. J Neurosci 20(20):7766–7775.

Nini A, Feingold A, Slovin H, Bergman H (1995) Neurons in the globus pallidus do not show correlated activity in the normal monkey, but phase-locked oscillations appear in the MPTP model of parkinsonism. J Neurophysiol 74(4):1800–1805.

Levy R, Ashby P, Hutchison WD, Lang AE, Lozano AM, Dostrovsky JO (2002) Dependence of subthalamic nucleus oscillations on movement and dopamine in Parkinson's disease. Brain 125:1196–1209.

Kuhn AA, Trottenberg T, Kivi A, Kupsch A, Schneider GH, Brown P (2005) The relationship between local field potential and neuronal discharge in the subthalamic nucleus of patients with Parkinson's disease. Exp Neurol 194:212–220.

Weinberger M, Mahant N, Hutchison WD, Lozano AM, Moro E, Hodaie M, Lang AE, Dostrovsky JO (2006) Beta oscillatory activity in the subthalamic nucleus and its relation to dopaminergic response in Parkinson's disease. J Neurophysiol 96:3248 –3256.

Moran A, Bergman H, Israel Z, Bar-Gad I (2008) Subthalamic nucleusf unctional organization revealed by parkinsonian neuronal oscillations and synchrony. Brain 131:3395–3409.

Kühn AA, Kupsch A, Schneider GH, Brown P. Reduction in subthalamic 8-35 Hz oscillatory activity correlates with clinical improvement in Parkinson's disease. Eur J Neurosci. 2006 Apr;23(7):1956-60.

Kühn AA, Tsui A, Aziz T, Ray N, Brücke C, Kupsch A, Schneider GH, Brown P. Pathological synchronisation in the subthalamic nucleus of patients with Parkinson's disease relates to both bradykinesia and rigidity. Exp Neurol. 2009 Feb;215(2):380-7.

Ray NJ, Jenkinson N, Wang S, Holland P, Brittain JS, Joint C, Stein JF, Aziz T. Local field potential beta activity in the subthalamic nucleus of patients with

Parkinson's disease is associated with improvements in bradykinesia after dopamine and deep brain stimulation. Exp Neurol. 2008 Sep;213(1):108-13.

Kühn AA, Kempf F, Brücke C, Gaynor Doyle L, Martinez-Torres I, Pogosyan A, Trottenberg T, Kupsch A, Schneider GH, Hariz MI, Vandenberghe W, Nuttin B, Brown P. High-frequency stimulation of the subthalamic nucleus suppresses oscillatory beta activity in patients with Parkinson's disease in parallel with improvement in motor performance. J Neurosci. 2008 Jun 11;28(24):6165-73.

Anzak A, Tan H, Pogosyan A et al. Subthalamic nucleus activity optimizes maximal effort motor responses in Parkinson's disease. Brain 2012;135 (Pt 9):2766–2778.

Beudel M, Little S, Pogosyan A, Ashkan K, Foltynie T, Limousin P, Zrinzo L, Hariz M, Bogdanovic M, Cheeran B, Green AL, Aziz T, Thevathasan W, Brown P. Tremor Reduction by Deep Brain Stimulation Is Associated With Gamma Power Suppression in Parkinson's Disease. Neuromodulation. 2015 Jul;18(5):349-54.

Anzak A, Gaynor L, Beigi M et al. A gamma band specific role of the subthalamic nucleus in switching during verbal fluency tasks in Parkinson's disease. Exp Neurol 2011;232:136–142.

Anzak A, Gaynor L, Beigi M et al. Subthalamic nucleus gamma oscillations mediate a switch from automatic to controlled processing: a study of random number generation in Parkinson's disease. Neuroimage 2013;64:284–289.

Deuschl G, Bain P, Brin M. Consensus statement of the movement disorder society on tremor. Ad Hoc scientific committee. Mov Disord 1998;13 (Suppl. 3): 2–23.

Mallet L, Schüpbach M, N'Diaye K, Remy P, Bardinet E, Czernecki V, Welter ML, Pelissolo A, Ruberg M, Agid Y, Yelnik J. Stimulation of subterritories of the subthalamic nucleus reveals its role in the integration of the emotional and motor aspects of behavior. Proc Natl Acad Sci U S A. 2007 Jun 19;104(25):10661-6.

Mandat TS, Hurwitz T, Honey CR. Hypomania as an adverse effect of subthalamic nucleus stimulation: report of two cases. Acta Neurochir (Wien). 2006 Aug;148(8):895-7; discussion 898.

Raucher-Chéné D, Charrel CL, de Maindreville AD, Limosin F. Manic episode with psychotic symptoms in a patient with Parkinson's disease treated by subthalamic nucleus stimulation: improvement on switching the target. J Neurol Sci. 2008 Oct 15;273(1-2):116-7.

Biseul I, Sauleau P, Haegelen C, Trebon P, Drapier D, Raoul S, Drapier S, Lallement F, Rivier I, Lajat Y, Verin M. Fear recognition is impaired by subthalamic nucleus stimulation in Parkinson's disease. Neuropsychologia. 2005;43(7):1054-9.

Vicente S, Biseul I, Péron J, Philippot P, Drapier S, Drapier D, Sauleau P, Haegelen C, Vérin M. Subthalamic nucleus stimulation affects subjective

emotional experience in Parkinson's disease patients. Neuropsychologia. 2009 Jul;47(8-9):1928-37.

van Rossum G, Python tutorial, Technical Report CS-R9526, Centrum voor Wiskunde en Informatica (CWI), Amsterdam, May 1995.

Cox, R.W., AFNI: What a long strange trip it's been, NeuroImage (2011).

Smith SM, Jenkinson M, Woolrich MW, Beckmann CF, Behrens TE, Johansen-Berg H, Bannister PR, De Luca M, Drobnjak I, Flitney DE, Niazy RK, Saunders J, Vickers J, Zhang Y, De Stefano N, Brady JM, Matthews PM. Advances in functional and structural MR image analysis and implementation as FSL. Neuroimage. 2004;23 Suppl 1:S208-19. Review.

D'Haese PF, Pallavaram S, Li R, Remple MS, Kao C, Neimat JS, Konrad PE, Dawant BM. CranialVault and its CRAVE tools: a clinical computer assistance system for deep brain stimulation (DBS) therapy. Med Image Anal. 2012 Apr;16(3):744-53.

Kasasbeh A, Abulseoud OA, Matsumoto JY, Stead SM, Goerss SJ, Klassen BT, Huston J 3rd, Min HK, Lee KH, Frye MA. Lack of differential motor outcome with subthalamic nucleus region stimulation in Parkinson's disease. J Clin Neurosci. 2013 Nov;20(11):1520-6.

Eisenstein SA, Koller JM, Black KD, Campbell MC, Lugar HM, Ushe M, Tabbal SD, Karimi M, Hershey T, Perlmutter JS, Black KJ. Functional anatomy of subthalamic nucleus stimulation in Parkinson disease. Ann Neurol. 2014 Aug;76(2):279-95.

Alkemade A, Schnitzler A, Forstmann BU. Topographic organization of the human and non-human primate subthalamic nucleus. Brain Struct Funct. 2015 Apr 29.